SESSION V

Non-Thermal Plasma and Urea Aftertreatment Technologies

Session Chair: Ken Howden
U.S. Department of Energy

NO_x CONVERSION CHEMISTRY IN PLASMA-ASSISTED CATALYSIS

B. M. Penetrante, R. M. Brusasco, B. T. Merritt, W. J. Pitz and G. E. Vogtlin
Lawrence Livermore National Laboratory

M. C. Kung and H. H. Kung
Center for Catalysis and Surface Science, Northwestern University

C. Z. Wan and K. E. Voss
Engelhard Corporation

ABSTRACT

A short background on the significance of NO_2 in lean-NO_x SCR is given. The mechanism of plasma oxidation of NO to NO_2 is then described. It is discussed why the plasma, by itself, cannot lead to the chemical reduction of NO_x to N_2 in lean-burn gas mixtures. The role of hydrocarbons in the plasma oxidation process is explained. In combination with some types of SCR catalyst, the plasma can greatly enhance the NO_x reduction. An example is presented to demonstrate the improvement in NO_x reduction efficiency that can be accomplished by combining a representative SCR catalyst with a plasma.

I. INTRODUCTION

Lean-burn engines have attracted considerable attention because of their high fuel efficiency and lower emission of carbon dioxide. These engines operate under net oxidizing conditions, thus rendering conventional three-way catalysts ineffective for controlling the NO_x emission. The NO_x in engine exhaust is composed primarily of NO; consequently, aftertreatment schemes have focused a great deal on the reduction of NO. Selective catalytic reduction (SCR) by hydrocarbons [1-2] is one of the leading catalytic aftertreatment technologies for the reduction of NO_x in lean-burn engine exhaust. In lean-NO_x SCR, the oxidation of NO to NO_2 serves an important role in enhancing the efficiency for reduction of NO_x to N_2.

II. SIGNIFICANCE OF NO_2 IN LEAN-NO_x SCR

Many studies suggest that lean-NO_x SCR proceeds via oxidation of NO to NO_2 by oxygen, followed by the reaction of the NO_2 with hydrocarbons [3-13]. On catalysts that are not very effective in catalyzing the equilibration of $NO+O_2$ and NO_2, the rate of N_2 formation is substantially higher when the input NO_x is NO_2 instead of NO. This has been observed on Na-ZSM-5 [9], Ce-ZSM-5 [9], $-Al_2O_3$ [3], H-ZSM-5 [3], ZrO_2 [14], and Ga_2O_3 [14]. It has also been observed that Group II metal oxides in general are much more effective in the SCR of NO_2 compared to NO [15].

The apparent bifunctional mechanism in the SCR of NO_x has prompted the use of mechanically mixed catalyst components, in which one component (for example, Mn_2O_3 or Mn_3O_4) is used to accelerate the oxidation of NO to NO_2 and another component (for example, Sn-ZSM-5 or In/Al_2O_3) catalyzes the reaction between NO_2 and the hydrocarbon [16-18]. Catalysts that previously were regarded as inactive for NO_x reduction could therefore become efficient when mixed with an oxidation catalyst.

The apparent role of NO_2 in the SCR of NO_x has also prompted the use of a multi-stage system in which an oxidation catalyst (for example, Pt-MFI zeolite) is used upstream of a reduction catalyst (for example, In-MFI or Zn-MFI zeolite) [19-20]. This latter method works fine particularly for systems that require hydrocarbon addition; the hydrocarbon can be injected between the oxidation catalyst and the reduction catalyst. For a lean-burn exhaust that already has a significant amount of hydrocarbons, the oxidation catalyst for NO is also active for the oxidation of the hydrocarbon; this results in a decrease in the efficiency of the hydrocarbon reductant.

It has been pointed out by Bethke et al. [21] and Chajar et al. [22] that the formation of gas phase NO_2 does not necessarily precede the formation of N_2. On catalysts such as Al_2O_3 that are less active in the oxidation of NO to NO_2, Bethke et al. [21] suggests that the N_2 production is higher using NO_2 than NO because of the higher surface coverage of adsorbed NO_2. The adsorbed NO_2 forms an adsorbed oxidized N-containing hydrocarbon intermediate. The reaction of this intermediate with NO is then the principal route to the production of N_2. For catalysts that deactivate

due to coking, NO_2 helps maintain the activity by removing the surface carbonaceous species, resulting in an impression that NO_2 is a reagent for N_2 production. In any case, it is apparent that preconverting NO to NO_2 opens the opportunity for a wider range of SCR catalysts and perhaps improves the durability of these catalysts.

III. PLASMA PROCESS

A non-thermal plasma [23-25] is a very effective means for oxidizing NO to NO_2 in the gas-phase under lean-burn engine exhaust conditions. The use of a plasma can improve the NO_x reduction efficiency and eliminate some of the deficiencies encountered in an entirely catalyst-based approach. The plasma can oxidize NO to NO_2 without depleting the amount of hydrocarbons available for SCR of NO_2 to N_2. The function of the SCR catalyst can thus be greatly simplified by focusing on the reduction of NO_2 by the hydrocarbon. Furthermore, the plasma can oxidize NO without oxidizing SO_2, thus making the process tolerant to the sulfur content of the fuel.

Previous studies [26-28] have shown that all electrical discharge plasma reactors produce a plasma with an average electron kinetic energy of around 3-6 eV. The plasma chemistry in discharge plasma reactors is therefore very similar regardless of electrode structure or the way the voltage is delivered to the reactor.

Plasma without Hydrocarbons - In the plasma, oxidation is the dominant process for exhausts containing dilute concentrations of NO in mixtures of N_2, O_2 and H_2O, particularly when the O_2 concentration is 5% or higher. The kinetic energy of the electrons is deposited primarily into the major gas components, N_2 and O_2. The most useful deposition of energy is associated with the production of N and O radicals through electron-impact dissociation:

$$e + N_2 \Rightarrow e + N(^4S) + N(^4S,^2D) \quad (1)$$

$$e + O_2 \Rightarrow e + O(^3P) + O(^3P,^1D) \quad (2)$$

where $N(^4S)$ and $N(^2D)$ are ground-state and metastable excited-state nitrogen atoms, respectively, and $O(^3P)$ (simply referred to as O) and $O(^1D)$ are ground-state and metastable excited-state oxygen atoms, respectively. The $N(^4S)$ is the only plasma-produced species that could effectively lead to the chemical reduction of NO [24,29]:

$$N(^4S) + NO \Rightarrow N_2 + O \quad (3)$$

In the presence of O_2, the oxidation pathway becomes dominant for two reasons:

(a) The dissociation energy of O_2 is smaller than that of N_2. For electrical discharge plasma reactors, the average electron kinetic energy is low, around 3-6 eV.[26-28] Under this condition the rate for dissociation of O_2 is much higher compared to the dissociation of N_2.[23-24] The dissociation of O_2 will produce only oxidative radicals. The ground-state oxygen atom, $O(^3P)$, will convert NO to NO_2 via

$$O(^3P) + NO + M \Rightarrow NO_2 + M \quad (4)$$

$$O(^3P) + O_2 + M \Rightarrow O_3 + M \quad (5a)$$

$$O_3 + NO \Rightarrow NO_2 + O_2 \quad (5b)$$

The metastable oxygen atom, $O(^1D)$, will react with H_2O to produce OH radicals:

$$O(^1D) + H_2O \Rightarrow 2\,OH \quad (6)$$

The OH radicals will convert NO and NO_2 to nitrous and nitric acid, respectively.

(b) High electron energies are required to optimize the production of $N(^4S)$ by electron-impact dissociation of N_2. Under conditions optimum for the dissociation of N_2, a large number of excited nitrogen atoms, $N(^2D)$, is produced [30-31]. The $N(^2D)$ species can lead to undesired reactions in the presence of O_2. Rather than reduce NO, the $N(^2D)$ species would react with O_2 to produce NO:

$$N(^2D) + O_2 \Rightarrow NO + O \quad (7)$$

Because of the large rate constant [32] for reaction (7) and the large concentration of O_2 relative to NO, the $N(^2D)$ species preferentially reacts with O_2 to produce NO. In a lean-burn exhaust, the production of NO by $N(^2D)$ will counterbalance the reduction of NO by $N(^4S)$, thus effectively leaving oxidation as the only pathway for NO conversion. The effect of $N(^2D)$ on the NO_x conversion chemistry has been validated in comparison with experiments [24].

The efficiency for oxidation of NO to NO_2 drops as the temperature is increased. At high temperatures, the NO to NO_2 oxidation reaction is counteracted by the reduction reaction:

$$O + NO_2 \Rightarrow NO + O_2 \quad (8)$$

Because of reaction (8), the oxidation of NO by the O radical is not efficient at high temperatures. We will show in the next section that the NO oxidation efficiency in the plasma can improve dramatically in the presence of hydrocarbons.

Plasma with Hydrocarbons - We next examine the effect of hydrocarbons on the plasma processing of NO. Propene was used as a representative hydrocarbon. The dry gas mixture contained 500 ppm NO in 10% O_2 and balance N_2. The purpose of this experiment was to determine how the hydrocarbon affects the plasma oxidation of NO to NO_2.

The NO_x concentrations for the cases without propene and with 1000 ppm propene are shown in Figures 1(a) and 1(b), respectively, for processing at 300°C.

For the case without propene (Figure1(a)), less than 20% of the NO is converted to NO_2 even at the high energy densities.

The number of NO molecules converted to NO_2 is determined by the number of O radicals produced by the plasma, not by the initial NO concentration. The number of O radicals is determined only by the energy density input to the plasma.

At high temperatures, the efficiency for conversion of NO to NO_2 is poor in the absence of hydrocarbons in the gas stream. Figure 1(b) shows the NO_x concentrations when 1000 ppm of propene is added to this gas stream. The main fate of NO in the plasma in the presence of hydrocarbons is the oxidation of NO to NO_2.

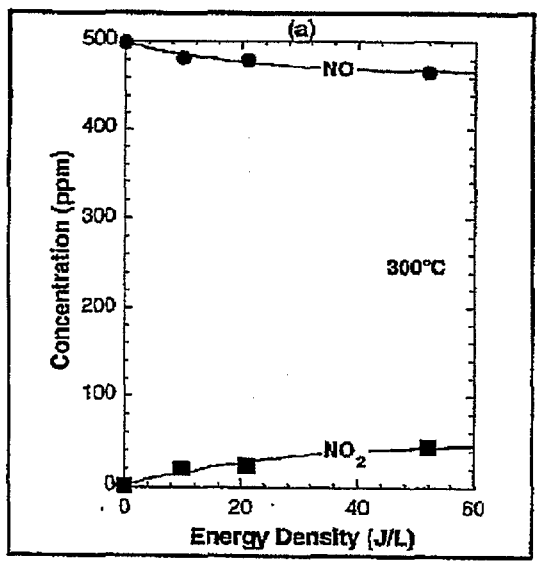

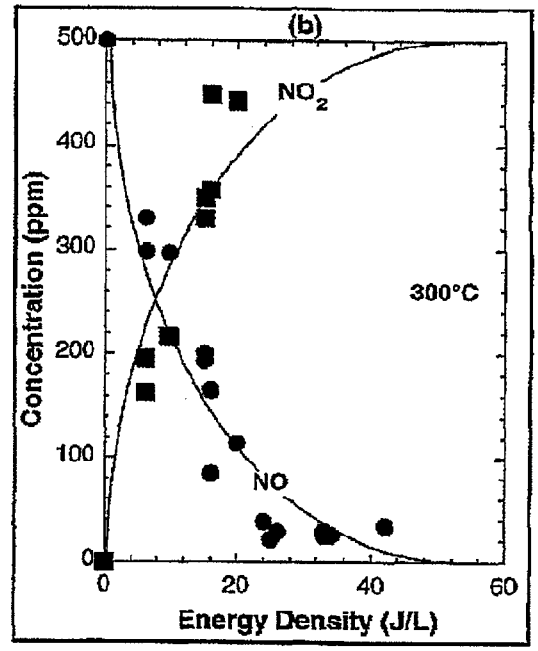

Figure 1. Effect of propene on the plasma oxidation of NO at 300°C. Plasma processing of 500 ppm NO in 10% O_2, balance N_2, (a) without propene, and (b) with 1000 ppm propene.

In the absence of hydrocarbons, the number of NO molecules oxidized to NO_2 is determined by the number of O radicals, which is proportional to the energy density input to the plasma. Backconversion of NO_2 to NO by the O radical via reaction (8) decreases the oxidation efficiency. In the presence of hydrocarbons, the radical responsible for the oxidation of NO to NO_2 is no longer the O radical. It will be shown in the following chemical kinetics analysis that the HO_2 is the radical that oxidizes NO to NO_2 when the plasma processing is done in the presence of hydrocarbons. The number of HO_2 radicals produced in the plasma is a function of both the energy density input to the plasma and the hydrocarbon concentration in the gas stream.

The experiments were interpreted with a detailed chemical kinetics model for propene oxidation [33-35] which included reactions to treat the plasma [23] and NO_x kinetics. Thermodynamic properties for the relevant radicals and stable parents were obtained by group additivity using THERM [36] with updated H/C/O groups and bond dissociation groups [37]. The thermochemical data allow accurate calculation of reverse reaction rate constants by microscopic reversibility. The C_3 mechanism was updated in a number of ways. The reactions involving propane were updated from Ref. [38].

The NO_x submechanism from GRI Mech [39] has been added to the C_3 mechanism. Most of the reaction rate constants were taken from Refs. [40] and [41].

In the very early stages of reaction the propene is mainly consumed by the O atom:

$$C_3H_6 + O \Rightarrow C_2H_5 + HCO \quad (9)$$

$$C_3H_6 + O \Rightarrow CH_2CO + CH_3 + H \quad (10)$$

$$C_3H_6 + O \Rightarrow CH_3CHCO + H + H \quad (11)$$

Abstraction reactions by O atoms do not contribute significantly to propene consumption at the low temperatures encountered in this study because of the higher activation energy of abstraction reactions compared to addition reactions.

Of the total reaction with O atom, reaction (9) contributes 50%, and reactions (10) and (11) contribute 25% each. The O atoms are consumed more effectively by reactions (9)-(11) than reactions (4) and (5): O + NO NO_2.

At 300°C and early in the reaction, about 98% of the O atoms react with propene compared to 2% with NO. The rate constants for propene + O are much faster than that for NO + O. This result means that the propene consumes most of the O atoms that might otherwise react with NO to form NO_2.

After the initial stages of reaction, the OH radical rather than O atom becomes the main radical consuming propene:

$$C_3H_6 + OH \Rightarrow C_3H_6OH \quad (12)$$

$$C_3H_6 + OH \Rightarrow C_3H_5 + H_2O \quad (13)$$

where the C_3H_5 radical symbolizes all three isomers, which were distinguished individually in the reaction mechanism. The switch from O atom reactions to OH reactions is mainly due to OH being produced by the reaction

$$NO + HO_2 \Rightarrow NO_2 + OH \quad (14)$$

Reaction (14) is also the main reaction that converts NO to NO_2.

In the presence of H_2O, electron-impact dissociation of H_2O would produce additional OH radicals. The metastable oxygen atom, $O(^1D)$, will react with H_2O to also produce OH radicals via reaction (6). These OH radicals will decompose the hydrocarbons, for example via reactions (12) and (13), and produce hydrocarbon radicals that convert NO to NO_2 in the presence of O_2.

The HO_2 radicals are also produced from reactions involving hydrocarbon intermediates of propene oxidation:

$$CH_2OH + O_2 \Rightarrow CH_2O + HO_2 \quad (15)$$

$$CH_3O + O_2 \Rightarrow CH_2O + HO_2 \quad (16)$$

$$HCO + O_2 \Rightarrow CO + HO_2 \quad (17)$$

$$H + O_2 \Rightarrow HO_2 \quad (18)$$

Therefore, the propene supplies HO_2 radicals that convert NO to NO_2. Without the propene, the main reaction to convert NO to NO_2 are reactions (4) and (5): O + NO NO_2. Radical-radical reactions involving O and OH (such as OH + O HO_2) are not important because of the low concentrations of these radicals.

Nearly all the O atoms for conversion are supplied by electron impact, which has an associated cost in electrical energy. The propene lowers the energy requirement by production of HO_2 radicals that then become the main radical for conversion of NO to NO_2.

The OH produced from reaction (6) can also react with NO and NO_2 to form their related acids:

$$NO + OH \Rightarrow HONO \quad (19)$$

$$NO_2 + OH \Rightarrow HONO_2 \quad (20)$$

At 300°C, during the time when the propene is being consumed most rapidly, only about 6% of the OH react with NO and NO_2 while the remainder react mostly with propene and its aldehydic intermediate products. At 100°C, 15% of the OH react with NO and NO_2, while the remainder react mostly with propene and aldehydic intermediates. The rate constants for the NO_x + OH reactions are much slower than for propene + OH reactions, so that OH reacts mainly with propene rather than NO and NO_2 [42].

Because the OH radical reacts preferentially with the hydrocarbon, the oxidation of NO_2 to nitric acid is minimized. If SO_2 is present in the exhaust, scavenging of the O and OH radicals by the hydrocarbons will also minimize the oxidation of SO_2 to SO_3.

The hydrocarbon serves important roles not only on the catalyst, but also in the plasma. For lean-burn gasoline engine exhausts, the hydrocarbons are already present - mostly in the form of

propene - typically at C_1 concentrations about six times that of NO. For diesel exhausts, the emitted gaseous hydrocarbon levels are much lower; however, the volatile organic fraction of the particulates could be a useful source of additional hydrocarbons.

The hydrocarbons play three important functions in the plasma: (1) the hydrocarbons lower the energy cost for oxidation of NO to NO_2, (2) the hydrocarbons minimize the formation of acid products, and (3) the hydrocarbons prevent the oxidation of SO_2 to SO_3.

IV. PLASMA-ASSISTED CATALYSIS

Process - The plasma-assisted catalytic reduction of NO_x is accomplished in essentially two steps. First, the plasma oxidizes NO to NO_2 in the presence of a hydrocarbon:

$$\text{plasma} + NO + HC + O_2 \Rightarrow NO_2 + \text{HC-products}$$

where HC refers to a hydrocarbon and HC-products refers to partially oxidized hydrocarbons. Second, the catalyst reduces NO_2 to N_2 by selective reduction using the hydrocarbons:

$$\text{catalyst} + NO_2 + HC \Rightarrow N_2 + CO_2 + H_2O.$$

There are three key features in the plasma-assisted catalytic reduction of NO_x.

- First, the plasma oxidation process is partial. This means the plasma oxidizes NO to NO_2 but does not further oxidize NO_2 to nitric acid. The plasma also produces some partially oxygenated hydrocarbons, but does not completely oxidize the hydrocarbons to CO_2 and H_2O. For some catalysts, the partially oxygenated hydrocarbons are much more effective compared to the original hydrocarbons in reducing NO_x to N_2.
- Second, the plasma oxidation process is selective. This means the plasma oxidizes NO to NO_2, but does not oxidize SO_2 to SO_3. This makes the plasma-assisted process more tolerant to the sulfur content of fuel compared to conventional lean-NO_x technologies.
- Third, by using a plasma to change the composition of NO_x from NO to NO_2, one can take advantage of a new class of catalysts that are potentially more durable and more active than conventional lean-NO_x catalysts.

Test Setup - Figure 2 shows one of the possible embodiments of the plasma-assisted catalyst processor. In this setup the plasma reactor is located upstream of the catalyst reactor. The same result is achieved if the catalyst is placed inside the plasma reactor.

The separate plasma/catalyst configuration shown in Figure 2 is very flexible. Although we have used a pulsed corona reactor, this type of reactor is not necessarily the only type that produces the same effect. It can be used with any type of plasma reactor and does not require a specific type of high-voltage power supply. All electrical discharge plasma reactors accomplish essentially the same gas-phase plasma chemistry for the same gas mixture [26-28].

The separate plasma/catalyst configuration is also very flexible with respect to the catalyst support structure. It can be used with a bed of catalyst pellets or a monolith. For monolith structures, any L/D (length/diameter) ratio can be accommodated.

Tests of the plasma/catalyst processor have been done using both a simulated exhaust gas mixture and a real exhaust from a Cummins B5.9 diesel engine.

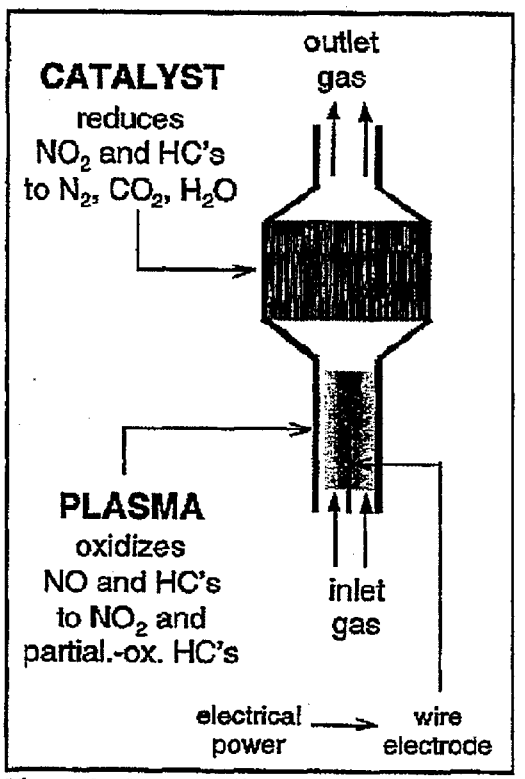

Figure 2. An embodiment of the plasma-assisted catalytic reduction process. The same result is achieved if the catalyst is placed inside the plasma reactor.

Catalyst- The aim of this paper is to demonstrate the improvement in NO_x reduction efficiency that can be accomplished by combining an SCR catalyst with a plasma. For this purpose we have chosen γ-Al_2O_3 as a representative SCR catalyst for three reasons. First, many groups have shown that γ-Al_2O_3 is much more active as an SCR catalyst for the reduction of NO_2 compared to NO [3,43-47]. γ-Al_2O_3 is one of the best non-proprietary materials for taking advantage of the presence of NO_2. Second, several studies [48-49] comparing a wide variety of SCR catalysts, including zeolites and metal oxides, have found γ-Al_2O_3 to be one of the most active for NO_x reduction by hydrocarbons. Third, γ-Al_2O_3 can be prepared in a hydrothermally stable form, thus making it a suitable catalyst or catalyst support for a practical device. Studies using a real diesel engine exhaust have shown that γ-Al_2O_3 retains its NO_x reduction activity over a long period of time [50].

Combining a plasma with γ-Al_2O_3 can provide NO_x reduction efficiencies much higher than those achieved by the conventional approach of loading a metal on γ-Al_2O_3. Figure 3(a) shows the NO reduction to N_2 for γ-Al_2O_3. The temperature operating window occurs at a high temperature and is narrow. The addition of 2 wt% Ag to γ-Al_2O_3 increases the NO reduction in the lower temperature region, as shown in Figure 3(b). When the input gas feed contains NO_2 instead of NO, the NO_x reduction activity over γ-Al_2O_3 increases dramatically over a wide range of temperature, as shown in Figure 3(c).

Figure 4(a) shows the NO reduction to N_2 for 2 wt% Co/Al_2O_3. With the same catalyst, the reduction activity in the lower temperature region is increased when the input gas feed contains NO_2 instead of NO, as shown in Figure 4(b). However, when NO_2 is used with pure γ-Al_2O_3, the NO_x reduction activity is higher over a much wider range of temperature, as shown in Figure 4(c).

Figure 5 shows the NO_x reduction to N_2 over a monolith washcoated with γ-Al_2O_3. The NO_x reduction is much higher when the input NO_x is NO_2 instead of NO.

Figures 3-5 illustrate how the conversion of NO to NO_2 can significantly increase the SCR activity. The gas feeds used were dry. It is known that H_2O degrades the SCR activity of γ-Al_2O_3. The negative effect of H_2O on the SCR activity of various catalysts, and how the effect can be overcome, is an important topic that is outside the scope of this paper. In the next section we will show the SCR activity of γ-Al_2O_3 for a real diesel engine exhaust, which contains about 5% H_2O.

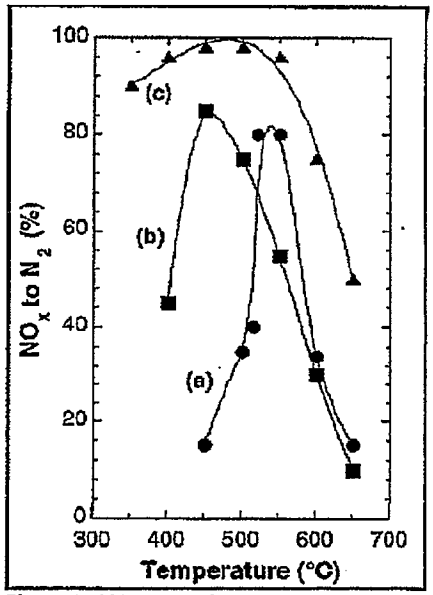

Figure 3. NO_x reduction to N_2 as a function of temperature. (a) NO over γ-Al_2O_3, (b) NO or NO_2 over 2 wt% Ag/Al_2O_3, (c) NO_2 over γ-Al_2O_3. Catalyst weight, 0.25 g. Dry gas feed, 1000 ppm NO or NO_2, 1000 ppm C_3H_6, 6% O_2, balance He at 100 mL/min. Space velocity = 12,000 /hr. Data taken from Ref. [46].

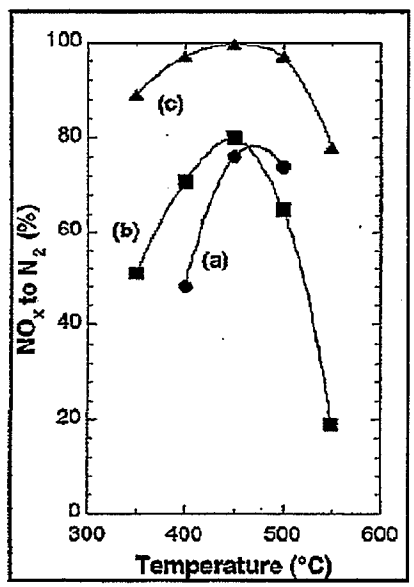

Figure 4. NO_x reduction to N_2 as a function of temperature. (a) NO over 2 wt% Co/Al_2O_3, (b) NO_2 over 2 wt% Co/Al_2O_3, (c) NO_2 over γ-Al_2O_3. Catalyst weight, 0.25 g. Dry gas feed, 1000 ppm NO or NO_2, 1000 ppm C_3H_6, 5% O_2, balance He at 100 mL/min. Space velocity = 12,000 /hr. Data taken from Ref. [47].

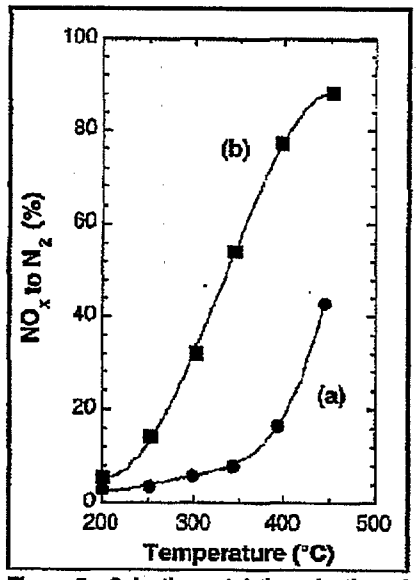

Figure 5. Selective catalytic reduction of NO_X over a monolith washcoated with γ-Al_2O_3. Space velocity = 18,000 /hr. L/D = 3. Dry gas feed. Gas mixture: 1000 ppm C_3H_6, 10% O_2, balance N_2. (a) input NO_X consisting of 500 ppm NO, (b) input NO_X consisting of 500 ppm NO_2.

Diesel Engine Exhaust Data - Figure 6 shows data on plasma-assisted catalytic reduction of NO_X using a slipstream of the exhaust from a Cummins B5.9 diesel engine. The reactor used in this run consisted of a pulsed corona plasma reactor packed with γ-Al_2O_3 pellets. The total plasma + catalyst reactor volume was 0.5 L. A Cummins B5.9 diesel engine running with a 95 kW load was used as the source of NO_X. The engine-out NO_X was 600 ppm. The exhaust temperature was typically between 350 - 400°C when the engine load is 95 kW. The temperature of the plasma/catalyst reactor was set at 370°C. Propene was used as the hydrocarbon reductant, with a C_1/NO_X ratio of 5. Figure 6 shows the amount of NO_X reduction at space velocities of 12,000 and 18,000 /hr. The NO_X reduction increases dramatically as the energy density delivered to the plasma is increased.

We have chosen γ-Al_2O_3 as a representative SCR catalyst that works very well in combination with a plasma. However, it is not necessarily the best catalyst for this purpose.

Actual exhaust from a diesel engine contains around 10% CO_2 and 5% or more H_2O, in addition to the 10% O_2. The H_2O component is known to decrease the SCR efficiency of γ-Al_2O_3. Some studies suggest that it is possible to overcome the detrimental effect of H_2O on SCR activity. For example, Maunala et al. [18] have observed that the activity of In/ Al_2O_3 remains high even in the presence of H_2O when the input NO_X is NO_2.

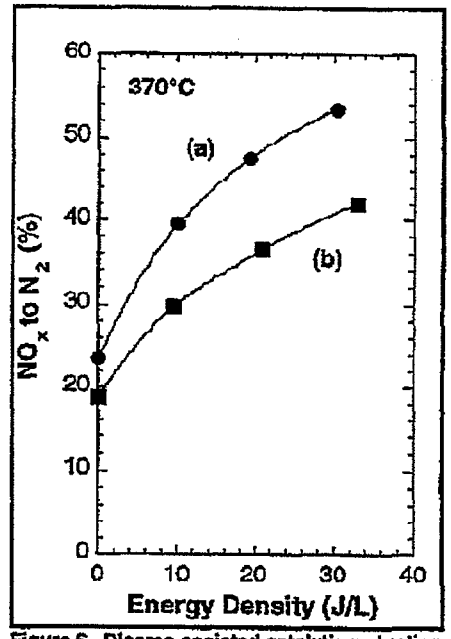

Figure 6. Plasma-assisted catalytic reduction of NO_X at 370°C in a pulsed corona plasma reactor packed with γ-Al_2O_3 pellets. Total plasma+catalyst reactor volume = 0.5 L. The NO_X reduction is shown as a function of the energy density input to the plasma. A Cummins B5.9 diesel engine running with a 95 kW load was used as the source of NO_X. Propene reductant $C_1/NO_X = 5$. Space velocity: (a) 12,000 /hr, and (b) 18,000 /hr.

V. CONCLUSIONS

The oxidation of NO to NO_2 serves an important role in enhancing the efficiency for SCR of NO_X to N_2. A non-thermal plasma is a very effective means for oxidizing NO to NO_2 in the gas-phase under lean-burn engine exhaust conditions. When combined with some types of SCR catalyst, the plasma can greatly enhance the NO_X reduction and eliminate some of the deficiencies encountered in an entirely catalyst-based approach. The plasma can efficiently oxidize NO to NO_2 over a wide range of temperature without depleting the amount of hydrocarbons available for SCR of NO_2 to N_2. Furthermore, in the presence of hydrocarbons the plasma can oxidize NO without oxidizing SO_2, thus making the process tolerant to the sulfur content of the fuel.

ACKNOWLEDGMENTS

The work at Lawrence Livermore National Laboratory was performed under the auspices of

the U.S. Department of Energy under Contract Number W-7405-ENG-48, with support from the Chemical Sciences Division of the DOE Office of Basic Energy Sciences, the DOE Office of Fossil Energy, the Strategic Environmental Research and Development Program, and a Cooperative Research and Development Agreement with Cummins Engine Company. The work at Northwestern University was supported by the Chemical Sciences Division of the DOE Office of Basic Energy Sciences.

REFERENCES

1. Shelef, M., "Selective Catalytic Reduction of NO_x With N-Free Reductants", *Chem. Rev.* **95**, 209 (1995).

2. Tabata, T., Kokitsu, M., and Okada, O., "Study on Patent Literature of Catalysts for a New NO_x Removal Process", *Catal. Today* **22**, 147 (1994).

3. Hamada, H., Kintaichi, Y., Sasaki, M., Ito, T., and Tabata, M., "Selective Reduction of Nitrogen Monoxide with Propane over Alumina and HZSM-5 Zeolite - Effect of Oxygen and Nitrogen Dioxide Intermediate", *Appl. Catal.* **70**, L15 (1991).

4. Petunchi, J.O. and Hall, W.K., "On the Role of Nitrogen Dioxide in the Mechanism of the Selective Reduction of NO_x over Cu-ZSM-5 Zeolite", *Appl. Catal. B: Environmental* **2**, L17 (1993).

5. Petunchi, J.O., Sill, G., and Hall, W.K., "Studies of the Selective Reduction of Nitric Oxide by Hydrocarbons", *Appl. Catal. B: Environmental* **2**, 303 (1993).

6. Valyon, J. and Hall, W.K., "Studies of the Surface Species Formed from NO on Copper Zeolites" *J. Phys. Chem.* **97**, 1204 (1993).

7. Sasaki, M., Hamada, H., Kintaichi, Y., and Ito, T., "Role of Oxygen in Selective Reduction of Nitrogen Monoxide by Propane over Zeolite and Alumina-Based Catalysts" *Catal. Lett.* **15**, 297 (1992).

8. Shelef, M., Montreuil, C.N., and Jen, H.W., "NO_2 Formation Over Cu-ZSM-5 and the Selective Catalytic Reduction of NO", *Catal. Lett.* **26**, 277 (1994).

9. Yokoyama, C. and Misono, M., "Catalytic Reduction of Nitrogen Oxides by Propene in the Presence of Oxygen over Cerium Ion-Exchanged Zeolites: 2. Mechanistic Study of Roles of Oxygen and Doped Metals", *J.Catal.* **150**, 9 (1994).

10. Bamwenda, G.R., Ogata, A., Obuchi, A., Takahashi, H., and Mizuno, K., "Selective Reduction of NO_2 by Propylene in Excess Oxygen Over Rh/Al_2O_3. Drift Spectroscopy and Activity Studies", *React. Kinet. Catal. Lett.* **56**, 311 (1995).

11. Lukyanov, D.B., Sill, G., Ditri, J.L., and Hall, W.K., "Comparison of Catalyzed and Homogeneous Reactions of Hydrocarbons for Selective Catalytic Reduction (SCR) of NO_x", *J.Catal.* **153**, 265 (1995).

12. Beutel, T., Adelman, B.J., Lei, G.D., and Sachtler, W.M.H., "Potential Reaction Intermediates of NO_x Reduction with Propane over Cu/ZSM-5", *Catal. Lett.* **32**, 83 (1995).

13. Ansell, G.P., Diwell, A.F., Golunski, S.E., Hayes, J.W., Rajaram, R.R., Truex, T.J., and Walker, A.P., "Mechanism of the Lean NOx Reaction over Cu/ZSM-5" *Appl. Catal. B* 2, 81 (1993).

14. Kung, M., Bethke, K., Alt, D., Yang, B. and Kung, H., in *NOx Reduction*, ACS Symposium Series (1995).

15. Shimokawabe, M., Ohi, A., and Takezawa, N., "Catalytic Reduction of Nitrogen Dioxide with Propene in the Presence and Absence of Oxygen Over Various Metal Oxides", *React. Kinet. Catal. Lett.* **52**, 393 (1994).

16. Hirao, Y., Yokoyama, C., and Misono, M., "Enhancement by Water Vapour of Catalytic Reduction of NO by Propene Over Mechanically Mixed Mn_2O_3 and Sn-ZSM-5", *Chem. Comm.* March 7, 597 (1996).

17. Misono, M., Hirao, Y., and Yokoyama, C., "Reduction of Nitrogen Oxides with Hydrocarbons Catalyzed by Bifunctional Catalysts", *Catal. Today* **38**, 157 (1997).

18. Maunala, T., Kintaichi, Y., Inaba, M., Haneda, M., Sato, K, and Hamada, H., "Enhanced Activity of In and Ga-Supported Sol-Gel Alumina Catalysts for NO Reduction by Hydrocarbons in Lean Conditions", *Appl. Catal. B: Environmental* **15**, 291 (1998).

19. Iwamoto, M., Hernandez, A.M., and Zengyo, T., "Oxidation of NO to NO_2 on a Pt-MFI Zeolite and Subsequent Reduction of NO_x by C_2H_4 on an In-MFI Zeolite: a Novel De-NO_x

Strategy in Excess Oxygen", *Chem. Comm.* Jan 7, 37 (1997).

20. Iwamoto, M. and Zengyo, T., "Highly Selective Reduction of NO in Excess Oxygen through the Intermediate Addition of Reductant (IAR) Between Pt- and Zn-MFI Zeolites", *Chem. Lett.* 1283 (1997).

21. Bethke, K.A., Li, C., Kung, M.C., Yang, B., et al., "The Role of NO_2 in the Reduction of NO by Hydrocarbon over Cu-ZrO_2 and Cu-ZSM-5 Catalysts", *Catal. Lett.* **31**, 287 (1995).

22. Chajar, Z., Primet, M., Praliaud, H., Chevrier, M., Gauthier, C., and Mathis, F., "Nitrogen Dioxide Effect in the Reduction of Nitric Oxide by Propane in Oxidizing Atmosphere", *Catal. Lett.* **28**, 33 (1994).

23. Penetrante, B.M., in "Non-Thermal Plasma Techniques for Pollution Control - Part A: Overview, Fundamentals and Supporting Technologies" (B.M. Penetrante and S.E. Schultheis, Eds.), p. 65. Springer-Verlag, Berlin Heidelberg New York, 1993.

24. Penetrante, B.M., Bardsley, J.N., and Hsiao, M.C., "Kinetic Analysis of Non-Thermal Plasmas Used for Pollution Control", *Jap. J. Appl. Phys.* **36**, 5007 (1997).

25. Penetrante, B.M., Hsiao, M.C., Bardsley, J.N., Merritt, B.T., Vogtlin, G.E., Kuthi, A., Burkhart, C.P., and Bayless, J.R., "Identification of Mechanisms for Decomposition of Air Pollutants by Non-Thermal Plasma Processing", *Plasma Sources Sci. Tech.* **6**, 251 (1997).

26. Penetrante, B.M., Hsiao, M.C., Merritt, B.T., Vogtlin, G.E., Wallman, P.H., Neiger, M., Wolf, O., Hammer, T. and Broer, S., "Pulsed Corona and Dielectric-Barrier Discharge Processing of NO in N_2", *Appl. Phys. Lett.* **68**, 3719 (1996).

27. Penetrante, B.M., Hsiao, M.C., Merritt, B.T., Vogtlin, G.E., Wallman, P.H., Kuthi A., Burkhart, C.P., and Bayless, J.R., "Electron-Impact Dissociation of Molecular Nitrogen in Atmospheric-Pressure Non-Thermal Plasma Reactors", *Appl. Phys. Lett.* **67**, 3096 (1995).

28. Penetrante, B.M., Hsiao, M.C., Merritt, B.T., Vogtlin, G.E. and Wallman, P.H., "Comparison of Electrical Discharge Techniques for Non-Thermal Plasma Processing of NO in N_2.", *IEEE Trans. Plasma Sci.* **23**, 679 (1995).

29. Penetrante, B.M., Hsiao, M.C., Merritt, B.T., and Vogtlin, G.E., "Fundamental Limits on NOx Reduction by Plasma", *SAE Paper* 971715 (1997).

30. Zipf, E.C., Espy, P.J. and Boyle, C.F., "The Excitation and Collisional Deactivation of Metastable N(^{2}P) Atoms in Auroras", *J. Geophys. Res.* **85**, 687 (1980).

31. Cosby, P.C., "Electron-impact Dissociation of Nitrogen", *J. Chem. Phys.* **98**, 9544 (1993).

32. Schofield, K., "Critically Evaluated Rate Constants for Gaseous Reactions of Several Electronically Excited Species", *J. Phys. Chem. Ref. Data* **8**, 723 (1979).

33. Wilk, R.D., Cernansky, N.P., Pitz, W.J. and Westbrook, C.K., "Propene Oxidation at Low and Intermediate Temperatures - A Detailed Chemical Kinetic Study", *Combust. Flame* **77**, 145 (1989).

34. Koert, D.N., Pitz, W.J. and Bozzelli, J.W., "Chemical Kinetic Modeling of High Pressure Propane Oxidation and Comparison to Experimental Results", Twenty-Sixth International Symposium on Combustion, The Combustion Institute, Pittsburgh, PA, 1996, p. 633-640.

35. Pitz, W.J., Westbrook, C.K. and Leppard, W.R., "Autoignition Chemistry of C4 Olefins Under Motored Engine Conditions: A Comparison of Experimental and Modeling Results", *SAE Paper 912315* (1991).

36. Ritter, E.R. and Bozzelli, J.W.," THERM - Thermodynamic Property Estimation for Gas Phase Radicals and Molecules", *Int. J. Chem. Kinet.* **23**, 767 (1991).

37. Lay, T.H., Bozzelli, J.W., Dean, A.M. and Ritter, E.R., "Hydrogen Atom Bond Increments for Calculation of Thermodynamic Properties of Hydrocarbon Radical Species", *J. Phys. Chem.* **99**, 14514 (1995).

38. Marinov, N.M., Castaldi, M.J., Melius, C.F. and Tsang, W., "Aromatic and Polycyclic Aromatic Hydrocarbon Formation in a Premixed Propane Flame", *Comb. Sci. Tech.* **28**, 295 (1997).

39. Bowman, C.T., Hanson, R.K., Davidson, D.F., Gardiner, Jr., W.C., Lissianski, V., Smith, G.P., Golden, D.M., Frenklach, M. and M.

Goldenberg, http://www.me.berkeley.edu/gri_mech, 1997.

40. Atkinson, R., Baulch, D.L., Cox, R.A., Hampson, Jr., R.F., Kerr, J.A. and Troe, J., "Evaluated Kinetic, Photochemical and Heterogeneous Data for Atmospheric Chemistry", *J. Phys. Chem. Ref. Data* **26**, 521 (1997).

41. Dean, A.M. and Bozzelli, J.W., "Combustion Chemistry of Nitrogen", in *Combustion Chemistry II*, ed. W. Gardiner, Jr. (Springer-Verlag, New York, 1997).

42. Pitz, W.J., Penetrante, B.M., Hsiao, M.C. and Vogtlin, G.E., "Simultaneous Oxidation of NO and Hydrocarbons in a Non-Thermal Plasma", *1997 Fall Meeting of the Western States Section of the Combustion Institute.*

43. Radtke, F., Koeppel, R.A., and Baiker, A., "Harmful By-Products in Selective Catalytic Reduction of Nitrogen Oxides by Olefins over Alumina", *Catal. Lett.* **28**, 131 (1994).

44. Kung, M., Lee, J.-H., Chu-Kung, A., and Kung, H.H., in "Proceedings, 11th International Congress on Catalysis-40th Anniversary" (J.W. Hightower, W.N. Delgass, E. Iglesia, and A.T. Bell, Eds), Vol. 101, p. 701. Elsevier, Amsterdam, 1996.

45. Radtke, F., Koeppel, R.A., Minardi, E.G., and Baiker, A., "Catalytic Reduction of Nitrogen Oxides by Olefins in the Presence of Oxygen over Copper/Alumina: Influence of Copper Loading and Formation of Byproducts", *J. Catal.* **167**, 127 (1997).

46. Bethe, K.A and Kung, H.H., "Supported Ag Catalyst for the Lean Reduction of NO with C_3H_6", *J. Catal.* **172**, 93 (1997).

47. Yan, J.-Y., Kung, M.C., Sachtler, W.M.H., and Kung, H.H., "Co/Al_2O_3 Lean NO_x Reduction Catalyst", *J. Catal.* **172**, 178 (1997).

48. Misono, M. and Kondo, K., "Catalytic Removal of Nitrogen Monoxide over Rare-Earth Ion-Exchanged Zeolites in the Presence of Propene and Oxygen", *Chem. Lett.* June, 1001 (1991).

49. Hamada, H., "Selective Reduction of NO by Hydrocarbons and Oxygenated Hydrocarbons over Metal Oxide Catalysts", *Catal. Today* **22**, 21 (1994).

50. Tabata, M., Tsuchida, H., Miyamoto, K., Yoshinari, T., et al., "Reduction of NO_x in Diesel Exhaust with Methanol over Alumina Catalyst", *Appl. Catal. B: Environmental* 6, 169 (1995).

PLASMA-CATALYSIS FOR DIESEL NOx REMEDIATION

John Hoard
Ford Motor Company

M. Lou Balmer
Batelle Pacific Northwest National Laboratory

ABSTRACT

A dielectric barrier discharge device has been built to test nonthermal plasma discharges for simulated diesel exhaust NOx removal. The device has also been tested with selected catalysts contained either in the plasma or after the plasma. The test stand and simulated diesel exhaust are described. Emissions are measured by conventional automotive emission analyzers, plus FTIR.

Dielectric barrier discharges without catalyst convert input NO to a mix of NO2, HONO, HNO3, and organic nitrates. O3 is not created when hydrocarbons are present. At 30 J/l energy deposition, approximately 29% of the input NO is "lost" -- i.e., not present in any components measured with the available instruments. Some of the propene and propane hydrocarbon input is converted to a variety of species, including CO, CO2, aldehydes, and alcohols.

Placing a Cu-ZSM catalyst after the plasma device at 180°C eliminates the apparent NOx conversion seen with the bare plasma. With this catalyst following the plasma, only slight NO conversion is seen, and all of the input NO is measured in the output sum of NO, NO2, HONO, and HNO3. This indicates that the apparent NOx conversion of the bare plasma is actually conversion to some (unmeasured) species which can be reconverted to NOx by the Cu-ZSM catalyst. It also indicates that background N2 does not participate in these low-power plasma discharges.

Placing a proprietary catalyst within the plasma results in significant NOx conversion. In this case, 50% of the input NO is not found in measured species after the plasma-catalyst system. Remaining NO is converted primarily to NO2. Placing a Cu-ZSM catalyst after this system does not degrade NOx efficiency.

It is concluded that significant NOx conversion can be obtained in lean exhaust by employing both the plasma discharge and an appropriate catalyst.

INTRODUCTION

Nonthermal plasma systems are being investigated for NOx removal in vehicle exhausts, particularly for diesel engines. This paper reports work done as part of a USCAR Low Emission Research and Development Partnership (LEP) CRADA in cooperation with Batelle Pacific Northwest National Lab (PNNL) and the Department of Energy (DOE).

TEST DEVICES

Dielectric barrier discharges are generated by the device shown in Figure 1. This consists of a pair of alumina plates, 18 mm wide by 90 mm long. The plates are bonded together with a 1.3 mm gap between them. Gold electrodes are coated onto the outside of the plates with wires bonded to them for external connection. The device is placed in a quartz tube which in turn is placed in an oven to control temperature. Gas blends are controlled by mass flow controllers.

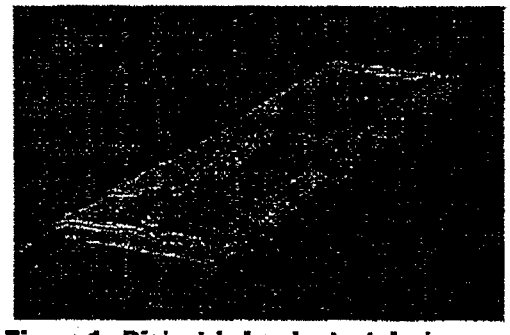

Figure 1. Dielectric barrier test device

These devices can have catalytic coating placed on their inner surfaces. However, for the data presented in this paper, catalyst materials have been coated on cordierite monoliths placed downstream of the plasma device. Two proprietary catalysts are used for this data:

- Cu-ZSM is a copper zeolite formulation provided by a catalyst supplier. The test piece is 25 mm long by 25 mm diameter.

- "A" is a proprietary catalyst formulation developed by the CRADA partners. The data shown here uses two pieces, each 25 mm long by 25 mm diameter.

Electrical power is delivered by a Trek 10/10 high voltage amplifier, driven by an HP function generator. For the data presented here, the input waveform is a triangular wave with peak voltage around 5.5 KV at 250 Hz frequency. Previous testing, not reported here, shows that the results are not sensitive to waveform for this device.

Unless otherwise noted, the test conditions are as shown in the following table.

ITEM	VALUE
Gas Composition	
NO	260 ppm
CO	400 ppm
H_2	133 ppm
Ar	1%
O_2	8%
CO_2	7%
C_3H_6	1575 ppm C_1
C_3H_8	525 ppm C_1
H_2O	7%
N_2	Balance
Temperature	180°C
Flow Rate	2 SLPM
Energy Deposition	30 J/l

Table 1. Test Conditions

The primary gas composition measurement is made using Ford's Real Time Emission Analyzer, which is based on an FTIR and provides measurement of as many as 23 gas concentrations at three second intervals. (1) Additional gasses can be analyzed by processing FTIR interferograms. Additional analysis equipment included a Beckman OM-11 oxygen analyzer, a Beckman Model 951 chemiluminescent NOx analyzer (CLA), a Beckman Model 400 FID hydrocarbon analyzer and Beckman Model 864 NDIR analyzers for CO and CO_2.

Conversion of NOx is measured as percent removal, comparing the inlet concentration to the outlet concentration. The REA FTIR measures NO, NO_2, HONO, NH_3, and N_2O. In addition, several other nitrogen-containing species are measured by analysis of the spectra. The CLA measures "NOx" by passing the sample gas over a heated catalyst and then through the chemiluminescent detection cell. The catalyst is designed to convert NO_2 to NO without conversion of NH_3 to NO. However, the efficiency of the catalyst and the accuracy of the detector cell are known to be affected by interference from other compounds, particularly formaldehyde. Thus, 25 ppm of formaldehyde (CH_2O) *is* expected to read as approximately 3.5 ppm NOx in the CLA. 32 ppm of methanol (CH_3OH) will read as 0.6 ppm NOx. The REA FTIR instrument has no such interference, and is used to measured CH_2O and CH_3OH in the present study.

In the following section, we will compare the NOx conversion efficiency as measured by several different analytical methods.

PLASMA-CATALYST RESULTS

Four configurations were tested in this study:

- The plasma device without a catalyst

- The plasma device followed by a Cu-ZSM catalyst

- The plasma device followed by catalyst "A"

- The plasma device followed by catalyst "A" followed by the Cu-ZSM catalyst

Figure 2 shows results for the bare plasma. Several gas concentrations are listed both with and without power to the plasma. The plasma converts nearly all of the input NO. A large fraction is converted to NO_2, with smaller quantities of N_2O, nitric- and nitrous- acid (about equal quantities) and methyl nitrate. "sumHC" is an REA FTIR measurement which uses generic hydrocarbon bands to measure the total HC concentration; it correlates well with FID measurement. The plasma partially oxidizes input HC. As usual in partial-oxidation processes, this results in CH_2O formation along with a large variety of hydrocarbon species.

Component	Formula	Plasma		Conversion %
		Off	On	
nitric oxide	NO	267	9	97
nitrogen diox.	NO2	6	170	
nitrous oxide	N2O	*	3	
acids	HONO+HNO3	*	4	
sumHC	"HC"	1937	1357	30
methyl nitrate	CH3ONO2	*	16	
methanol	CH3OH	*	3	
formaldehyde	CH2O	*	127	
Sum N species		276	205	26
CLA NOx		265	218	18
CLA Adj. CH2O, CH3OH		265	188	29
*Below detection limit				

Figure 2. Test results for plasma device without catalyst. Concentrations are ppm.

NOx conversion is calculated at the bottom of the figure, in three different ways. First, the concentrations of all the nitrogen-containing species as measured by the REA FTIR are added. Next, the CLA unadjusted NOx reading are and compared to the CLA readings that are adjusted for the presence of CH_2O and CH_3OH. It can be seen that the uncorrected CLA measurement gives significantly lower NOx efficiency. The corrected CLA measurement agrees well with the REA FTIR data.

Figure 3 shows FTIR spectra taken during this test. The upper trace is with the plasma power off. The second trace has the plasma power on. The third trace is the difference between the top two; that is, a spectrum of the products of the plasma operation. C_3H_6 (the large peak just above 900 cm^{-1}) has also been subtracted out of this trace for clarity. The fourth trace is a reference spectrum of methyl nitrate, CH_3ONO_2, which was taken at Ford Research Labs by Tim Wallington and his co-workers. The bottom trace is a reference spectrum of methanol, CH_3OH. It is readily apparent from these traces that methyl nitrate is formed in the plasma.

Figure 4 shows test results for the plasma followed by CuZSM catalyst. Unlike the bare plasma, in this case the NO is largely unconverted. Since the plasma device is unchanged, this means that the CuZSM has reconverted the plasma reaction products back to NO. Note that the acids and methyl nitrate are also reconverted. There is essentially no reduction of NOx to N2 over this combination.

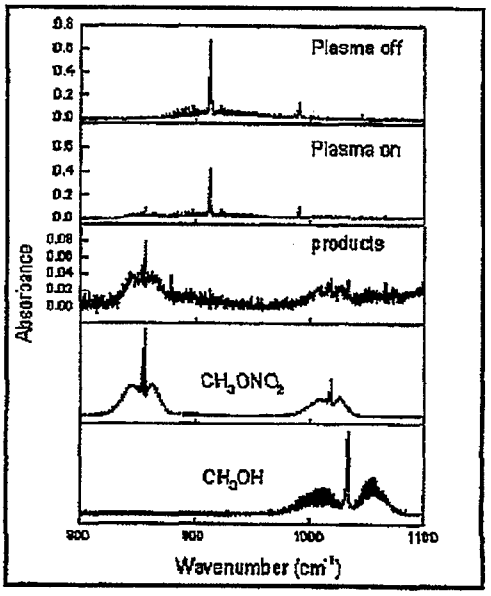

Figure 3. FTIR spectra for the plasma without catalyst.

Component	Formula	Plasma		Conversion %
		Off	On	
nitric oxide	NO	284	260	8
nitrogen diox.	NO2	*	*	
nitrous oxide	N2O	*	3	
acids	HONO+HNO3	*	*	
sumHC	"HC"	1878	1952	28
methyl nitrate	CH3ONO2	*	*	
methanol	CH3OH	*	23	
formaldehyde	CH2O	6	136	
Sum N species		281	267	5
CLA NOx		261	253	3
CLA Adj. CH2O, CH3OH		260	215	17
*Below detection limit				

Figure 4. Test results for plasma device followed by Cu-ZSM catalyst.

Note also that in Figure 2 an apparent NOx conversion of 29% is measured. That is, the combination of CLA and FTIR did not detect the fate of 29% of the input NO. In the absence of other analytical data this NO loss may have been interpreted as NO reduction to N_2. However, since the NO reappears over the CuZSM, it is apparent that in fact the conversion is to some other, unmeasured, product.

Figure 5 shows results for the plasma device followed by the proprietary catalyst "A". With this catalyst, virtually all of the remaining NOx

is in the form of NO. There are no detectable acids or nitrates. As befcre, HC is partially oxidized and CH_2O and CH_3OH are formed. NOx conversion is about 50%. Again, note the low measurement of conversion by the uncorrected CLA.

Component	Formula	Plasma		Conversion %
		Off	On	
nitric oxide	NO	280	117	58
nitrogen diox.	NO2	*	3	
nitrous oxide	N2O	*	*	
acids	HONO+HNO3	*	*	
sumHC	"HC"	1932	1335	31
methyl nitrate	CH3ONO2	*	*	
methanol	CH3OH	*	24	
formaldehyde	CH2O	7	146	
Sum N species		286	142	50
CLA NOx		290	176	39
CLA Adj. CH2O, CH3OH		290	137	53
*Below detection limit				

Figure 5. Test results for plasma device followed by proprietary catalyst "A"

Figure 6 shows the FTIR spectra for gas samples taken downstream from both the plasma and the proprietary catalyst. When these spectra are compared to the FTIR results shown in Figure 3, where there was no catalyst after the plasma, it can be seen that after the proprietary catalyst the methyl nitrate product is reduced to insignificant quantities.

Figure 7 shows test results for plasma followed by catalyst "A" followed by CuZSM catalyst. Unlike the second case, where the apparent NOx efficiency of the bare plasma is turned off by the CuZSM, in this case the CuZSM reduces measured NOx efficiency only a small amount. It cannot be concluded that the product is N_2, but it can be concluded that the CuZSM does not convert any products back to NOx.

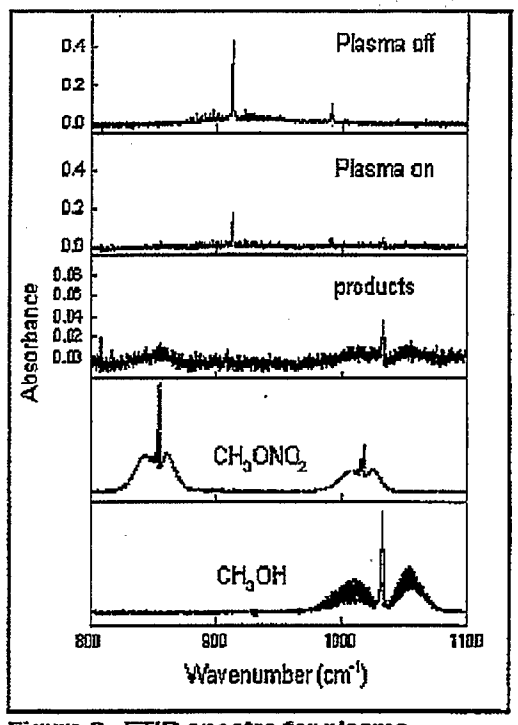

Figure 6. FTIR spectra for plasma followed by catalyst "A"

Component	Formula	Plasma		Conversion %
		Off	On	
nitric oxide	NO	277	141	49
nitrogen diox.	NO2	*	*	
nitrous oxide	N2O	*	6	
acids	HONO+HNO3	*	*	
sumHC	"HC"	1613	1225	32
methyl nitrate	CH3ONO2	*	*	
methanol	CH3OH	*	22	
formaldehyde	CH2O	8	131	
Sum N species		279	152	46
CLA NOx		277	185	33
CLA Adj. CH2O, CH3OH		276	148	46
*Below detection limit				

Figure 7. Test results for plasma followed by catalyst "A" followed by CuZSM.

NOx conversion results are summarized in Table 2. It can be seen that the CLA consistently underestimates NOx conversion, primarily due to the interference from formaldehyde.

Config.	$NO + NO_2$ + HONO	All "N" Species	CLA	CLA adj. for
Plasma Without	34	29	16	29
Plasma - CuZSM	8	5	3	17
Plasma - "A"	55	50	39	53
Plasma - "A" -	49	46	33	46

Table 2. Summary of NOx conversion for four test configurations and four NOx measurement techniques.

NO_2 VERSUS NO INPUT

It has been speculated (for instance, Penetrante et.al., (3)) that an important mechanism of plasma-catalyst reactions is conversion of NO to NO_2 in the plasma, followed by heterogeneous reaction of NO_2 with HC over a catalyst. As a test of this hypothesis, we replaced the NO in our feed stream with an equal amount of NO_2. The same plasma test device and proprietary catalyst "A" (but not CuZSM) were used. Figure 8 shows HC and NOx conversion efficiency with NO_2 and NO as the input. The left most pair of bars is for the NO_2 feed with plasma power off. The second set is NO_2 with plasma power on. The third set is for the NO feed with power off, and the final pair is NO with plasma power on. It can be seen that there is no NOx conversion when the input gas is NO_2, either with or without plasma power. HC conversion is roughly the same with power on, with either NO or NO_2 input.

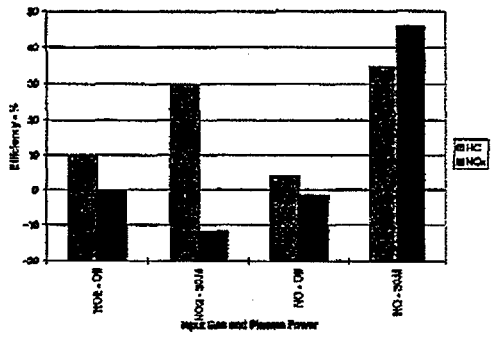

Figure 8. HC and NOx conversion with NO_2 versus NO, with and without plasma power.

Figure 9 shows NO and NO_2 concentrations for six conditions. The left most pair of bars shows NO_2 input with flow bypassed around the reactor and catalyst. This shows, as expected, that all the NOx is NO_2 in the input. The second pair of bars shows NO_2 input, power off, flow through the reactor and catalyst. The catalyst converts about 30% of the NO_2 to NO, but the sum $(NO+NO_2)$ is constant. The third set of bars is for the same input conditions as the second set and shows essentially no change when the plasma power is turned on. The fourth set of bars is for NO input, bypassing the reactor. There is slight conversion of NO to NO_2 in the heated stainless steel lines. The fifth set of bars shows NO input, power off, flow through the reactor. There is no difference in output concentrations between this and the bypass condition. The final pair of bars where conditions are NO input with power on and flow through the plasma and catalyst about 50% NOx reduction, and most of the remaining NOx as NO.

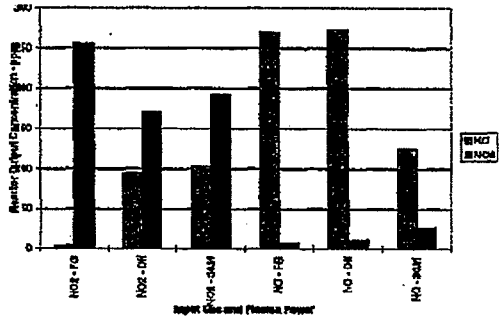

Figure 9. NO and NO_2 concentrations in ppm.

These results indicate that for catalyst "A" the NOx reduction is not a simple reaction between NO_2 and HC over the catalyst. With or without plasma, NO_2 input does not result in net NOx reduction. Since earlier data showed that the bare plasma coed indeed convert NO to NO2, then it is apparent that there are important species created in the plasma in addition to the NO_2 that play a key role in the reduction reaction and that are not created when NO_2 is passed through the catalyst without the plasma. Further work is needed to fully understand this phenomenon.

CONCLUSION

- In these experiments, plasma without a catalyst does not give real NOx reduction, only conversion to a variety of species which can be reconverted to NOx by CuZSM catalyst at 180°C.

- A suitable catalyst such as "A" can produce larger conversion, and the products are not reconverted by CuZSM

- Plasmas can create a wide variety of reaction products, including CH_2O, CH_3OH, and CH_3ONO_2.

- Use of standard chemiluminescent NOx analyzer can lead to incorrect measurement of NOx efficiency if interference species are present. Suitable instrumentation needs to be used to reduce this possibility.

- The NOx reduction mechanism is more complicated than a simple NO_2 selective catalytic reduction with HC. Further work is needed to elucidate the mechanism.

ACKNOWLEDGMENTS

The authors wish to acknowledge significant contributions by our co-workers at Ford Research Lab, Batelle Pacific Northwest National Laboratory, General Motors Delphi, and Chrysler Corporation. Special thanks is given to Dr. Tim Wallington at Ford Research for his help in analyzing FTIR spectra and providing reference spectra, and to Chris Gierczak and Tom Korniski of Ford Research for their help in operation and maintenance of the REA FTIR.

Support for Dr. M. Lou Balmer was provided by the DOE Energy Efficiency Office of Advanced Automotive Technology.

REFERENCES

1. "FTIR: Fundamentals and applications in the analysis of dilute vehicle exhaust"; C. A. Gierczak, J. M. Andino, J. W. Butler, G. A. Heiser, G. Jession, and T. J. Korniski, *SPIE - The International Society for Optical Engineering*, volume 1433 Measurement of Atmospheric Gases (1991), p. 315ff.

2. "Investigation of Analyzer Problems in the Measurement of NOx from Methanol Vehicles", Peter A. Gabele, EPA report number PB89-124374, November 1988.

3. "Plasma-Assisted Heterogenous Catalysis for NOx Reduction in Lean-Burn Engine Exhaust", B.M. Penetrante, M.C. Hsaio, B.T. Merritt, G.E. Voigtlin, C.Z. Wan, G.W. Rice, K.E. Voss, Proceedings of the 1997 Diesel Engine Emission Reduction Workshop.

NITROGEN MEASUREMENT FROM NOx REDUCTION FOR A PLASMA CATALYST SYSTEM IN SIMULATED DIESEL EXHAUST

M. Lou Balmer, Russ Tonkyn, and I. Steven Yoon
Pacific Northwest National Laboratory

John Hoard
Ford Motor Company

ABSTRACT

Recent work has shown that energy efficiencies as well as yields and selectivities of the NO_x reduction reaction can be enhanced by combining a plasma discharge with select catalysts. While analysis of gas phase species with a chemiluminescent NO_x meter and mass spectrometer shows that significant removal of NO_x is achieved, high background concentrations of nitrogen preclude the measurement of nitrogen produced from NO_x reduction. Results presented in this paper show that N_2 from NO_x reduction can be measured if background N_2 is replaced with helium. Nitrogen production results are presented for a catalyst system where the catalyst is in the plasma region and where the catalyst is downstream from the plasma. The amount of N_2 produced is compared with the amount of NO_x removed as measured by the chemiluminescent NO_x meter. Considerable variation in the amount of N_2 measured as a result of NOx reduction has been observed. The measured nitrogen from NO_x reduction accounts for 71±5% of the total NO_x removed in a single stage configuration and 50±6% for a two stage configuration. Analysis of product gases by Fourier transform infrared spectroscopy revealed that species such as, N_2O, HONO, HNO_3, NO_2, and CH_3ONO_2 are not present in detectable quantities.

INTRODUCTION

Non-thermal dielectric barrier discharge systems are being examined for reduction of nitrogen oxides in diesel and lean burn vehicle exhaust. While theoretical and experimental work has shown that gas phase discharges can lower NO_x and hydrocarbon concentrations in simulated vehicle exhaust, the energy efficiency and selectivity is low. [1,2] Recent work has shown that energy efficiencies as well as yields and selectivities of the NO_x reduction reaction can be enhanced by combining the discharge with select material surfaces. [2,3]
Diesel and lean burn exhausts contain a complex mixture of components that contribute to the overall chemistry promoted in the gas phase and on the surfaces of catalysts. The interactions between hydrocarbons, NO_x, water, oxygen, and hydroxyl radicals created in the plasma can potentially lead to a number of unwanted reaction by-products such as NO_2, N_2O, HONO, HNO_3, CH_2O and organo-nitrates.

Direct detection of N_2 from the reduction of NO_x has not been demonstrated due to high concentrations of N_2 in the exhaust streams and relatively minute starting concentrations of NO (50-500 ppm). Therefore, reported NO_x reduction is derived from the amount of NO_x that "disappears" and which is not detected as other by-product species. Potentially large errors in the amount of NO_x "reduced" can occur if the appropriate suite of analysis equipment is not used to measure all product gases or if surface adsorbed NO_x is not measured.

The purpose of the study described in this paper is to determine if nitrogen from NO_x reduction can be detected and quantified downstream of a plasma catalyst system that shows apparently high NO_x reduction efficiency. An earlier study [4] using the same catalyst found that only 45% of NOx that disappeared was converted to nitrogen, however, quantification of nitrogen was affected by large variations in background nitrogen concentrations. In this study background nitrogen levels were dramatically reduced and quantification techniques were improved.

EXPERIMENTAL

A proprietary catalyst was tested in two configurations. In the first configuration, the catalyst is in the discharge region in a dielectric barrier packed bed reactor. In the second configuration, the catalyst is placed downstream from the region in which the discharge occurs. These two configurations are shown schematically in Figure 1.

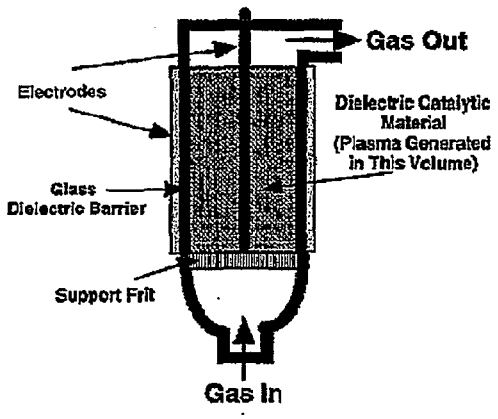

Figure 1a: Single-stage reactor configuration where the catalyst is tested in the plasma region.

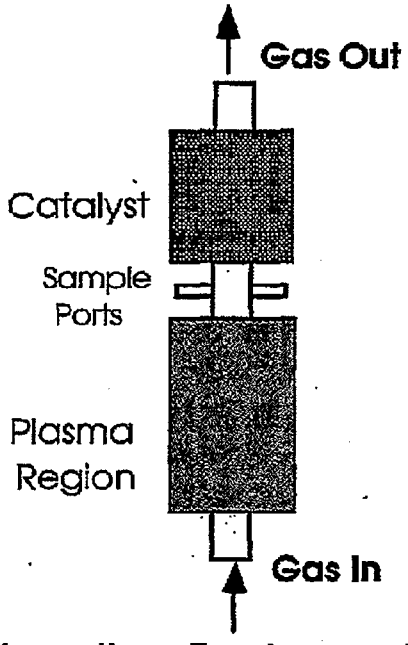

Figure 1b: Two-stage reactor configuration where the catalyst is downstream from the plasma reactor.

A dielectric barrier packed bed reactor described in Tonkyn et al. [2] was used to generate the plasma. The feed gas conditions were varied for each experiment and are described in the results section. The product gases were analyzed with a chemiluminescent NO_x analyzer (CLA), a mass spectrometer, and a gas chromatograph (gc).

The power deposited into the reactor was measured with a capacitive circuit and a high voltage probe. [2] The beta (β) parameter, which is used to characterize the energy efficiency of the discharge treatment, is represented as follows:

$$[NO_x] = [NO_x]_f + ([NO_x]_o - [NO_x]_f) * e^{-E/\beta}$$

where β is the first order decay parameter in Joules/standard liter, $[NO_x]_o$ is the initial NOx concentration and $[NO_x]_f$ is the final limiting NO_x concentration.

RESULTS AND DISCUSSIONS

Two experiments were conducted using the single-stage configuration shown in Figure 1a. In the first experiment the exhaust gas mix simulated diesel and lean burn conditions with the following concentration of gases: 250 ppm NO, 525 ppm C_3H_6, 75 ppm C_3H8, 7% H_2O, 8% O_2, 7% CO_2, 9000 ppm Ar, 400 ppm CO, 130 ppm H_2, and nitrogen balance. The temperature was maintained at 180EC and the gases were flowed at 4 L/min to give an hourly space velocity of 12,000 hr^{-1} over the catalyst. The NO and NO_x concentrations as a function of input energy as measured by the CLA are shown in Figure 2. The difference in NO and NO_x measurement is the amount of NO that is oxidized to NO_2. The data show that a maximum of 67% of NO_x is removed and presumably reduced to N_2.

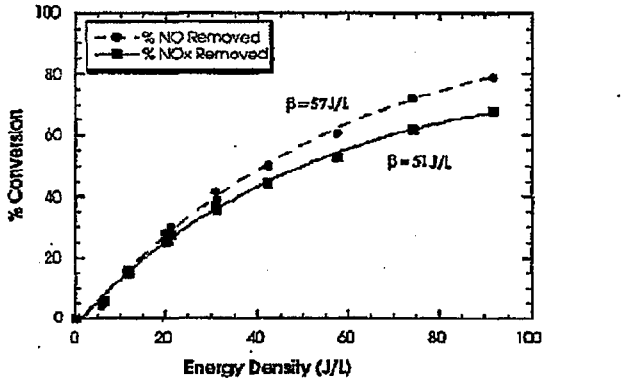

Figure 2: NO_x conversion as a function of input energy for a lean NO_x gas mixture at 180°C and 12,000 hsv.

In the second set of experiments the N_2 carrier gas was replaced with He so that N_2 from NO reduction could be detected using a gas chromatograph and mass spectrometer. The gas mix contained less CO_2 (4%) and water (2%) than the mix with the nitrogen carrier. Removal of CO, CO_2, H_2 and Ar from the gas stream does not affect the distribution of NO and NO_x in the have shown that hydrocarbon and oxygen concentrations do affect the NO_x reduction product gas stream. Earlier unpublished results chemistry in similar plasma/catalyst systems. In

addition, the presence of water affects the chemistry in the range of 0-2%, however, no change in product distribution is observed with increasing water concentration above 2%. The temperature and space velocity was 200EC and 9000 hr^{-1} respectively. Figure 3 shows the percent of NO and NO_x removed as a function of input energy for this mixture.

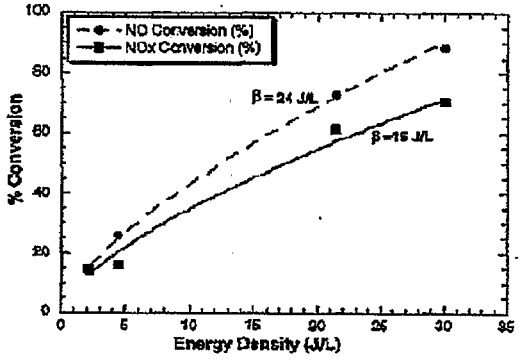

Figure 3: NO_x conversion as a function of input energy for a gas mixture containing, 250 ppm NO, 700 ppm C_3H_6, 8%)$_2$, 9% H_2O and balance He.

Comparison of Figure 2 and Figure 3 reveals that while the energetics of NO_x destruction are more efficient in the He mixture, the product distribution (NO and NO_x) appears to be similar. It is worth noting that this result does not prove that the predominant chemical mechanisms in He and N_2 carrier gases are the same.

For the gas mix with the He carrier, the nitrogen concentration in the exhaust from the reactor was monitored using a gas chromatograph equipped with a thermal conductivity detector. A 5Å molecular sieve column on the gas chromatograph was used to separate N_2 and O_2.

Figure 4 shows the area under the nitrogen peak as a function of time with the plasma on (energy deposited at 22 J/L) and the plasma off. Figure 5 shows the corresponding NO and NO_x concentrations as measured by the chemiluminescent NO_x meter. It can be seen in Figure 4 that when the plasma is initiated (100 min), the nitrogen signal increases significantly and a corresponding decrease in NO_x is measured by the NO_x meter. There is a slow rise in nitrogen concentration over the first 50 minutes after which the nitrogen concentration remains constant. When the plasma is turned off (300 min.), the N_2 drops to the background level and the NO_x returns to its original concentration.

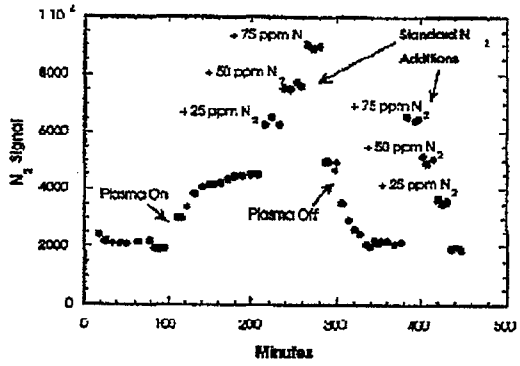

Figure 4: N_2 production measured by the gas chromatograph downstream from a catalyst in plasma with He carrier gas.

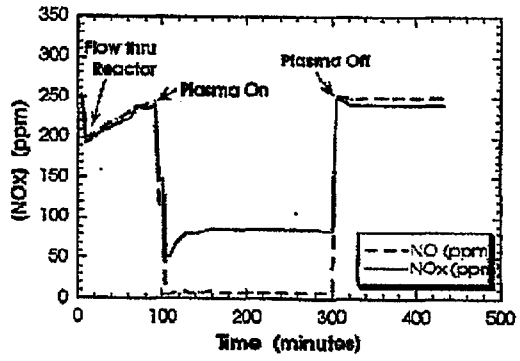

Figure 5: NO_x removal in He as measured by the chemiluminescent NO_x meter. This data corresponds to N_2 production illustrated in Figure 4.

If the propylene is turned off with the plasma on (data not shown), the N_2 drops slowly back to baseline concentrations over a 25 minute time period and the NO and NO_x concentration increases concomitantly. This indicates that 1.) propylene is necessary for NOx reduction, and that 2.) there is storage of propylene on the surface which continues to react to reduce NOx to N_2 until the propylene is depleted.

Standard additions of 25, 50, and 75 ppm of N_2 were added to the lean mix with the plasma on and off to calibrate the gas chromatograph andquantify the concentration of N_2. The response of the gc as a function of nitrogen concentration is plotted in Figure 6 for the plasma on and the plasma off. It is hypothesized that the difference in slope of the two lines is due to a minor amount of nitrogen radical formation from

N_2 when the plasma is on. The slope of the line with the plasma on was used to calculate the amount of nitrogen formed by the plasma to account for N! formation from N_2 produced from NOx reduction.

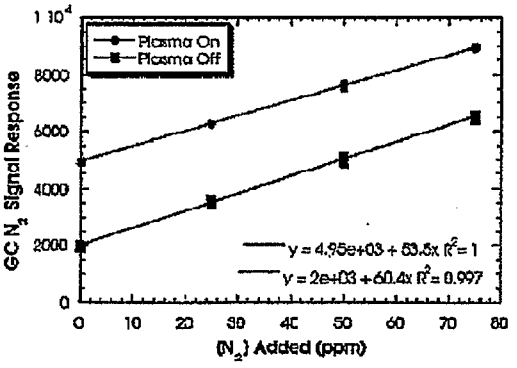

Figure 6: Gas chromatograph calibration curve for standard nitrogen additions with the plasma off and the plasma on.

The slope of the line with the plasma off was used to calculate the background concentration of nitrogen. From this, 59 ppm of N_2 is formed with a corresponding NO_x loss as measured by the NO_x meter of 155 ppm. Therefore, if all of the removed NO_x is converted to N_2, 77.5 ppm of N_2 should be produced. Comparing this value to the amount of nitrogen detected, 76% of the NO_x removed can be accounted for as nitrogen.A similar set of experiments was performed for the configuration where the catalyst is downstream from the plasma reactor (two-stage). For this configuration the catalyst was coated onto a cordierite honeycomb monolith which was placed downstream from the plasma reactor. Gas samples were taken between the reactor and the catalyst bed and downstream from the catalyst bed. Figure 7 shows the NO_x destruction efficiency as a function of energy deposited in the reactor for the two-stage configuration before and after the catalyst. The reactor temperature was 180EC and the catalyst temperature was 150EC. The gas mixture contained 7.5% oxygen, 4% CO_2, 2% water, 0.2% CO, 750 ppm C_3H_6 and 270 ppm NO. The space velocity was 7500 hr^{-1}. Note that this mix contains less water than that used for the single-stage tests.

As illustrated in Figure 7a, the primary effect of the plasma is to convert NO to NO_2 with little apparent reduction of NO_x. Also, mass spectrometer measurements (not shown) indicate that the propylene is partially, but not completely, oxidized over the energy range tested. These results are similar to results published in the literature. [3,5] The maximum apparent NO_x reduction is 60% downstream from the catalyst bed, (Fig. 7b) which is similar to the value obtained for the single-stage reactor, however, energy efficiency is about ten times higher in the 2-stage configuration.

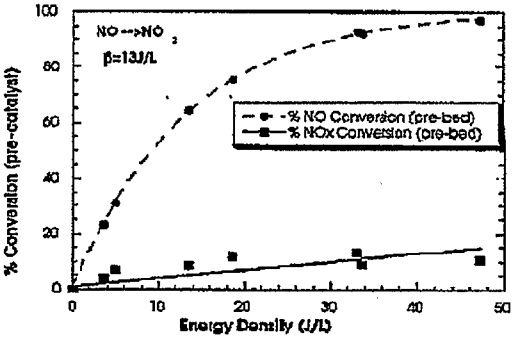

Figure 7a: NO_x destruction efficiency in a simulated lean NO_x mixture after the plasma reactor but before the catalyst bed.

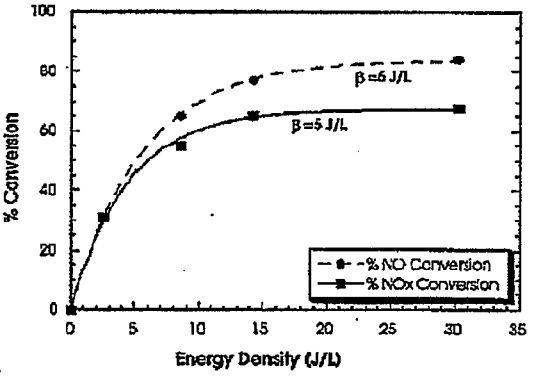

Figure 7b: NO_x destruction efficiency downstream from both the reactor and the catalyst bed.

The NO_x removal efficiency for the two-stage reactor configuration in a helium carrier with 7.5% oxygen, 2% water, 750 ppm C_3H_6, and 270 ppm NO at a space velocity of 7500 hr^{-1} is illustrated in Figure 8. Again, the product distribution (NO and NO_x) in the He mix and in the N_2 lean burn mix are the same, with higher energy efficiency in the He mix.

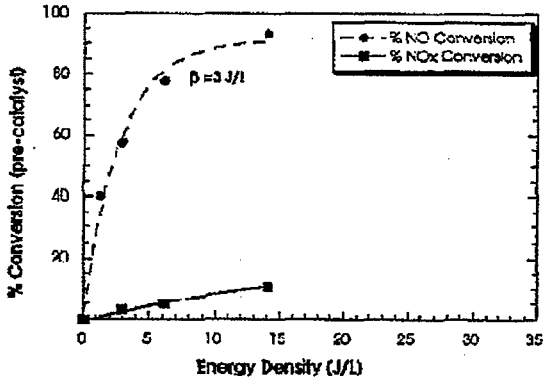

Figure 8a: NO_x destruction efficiency in a He mixture after the plasma reactor and before the catalyst bed.

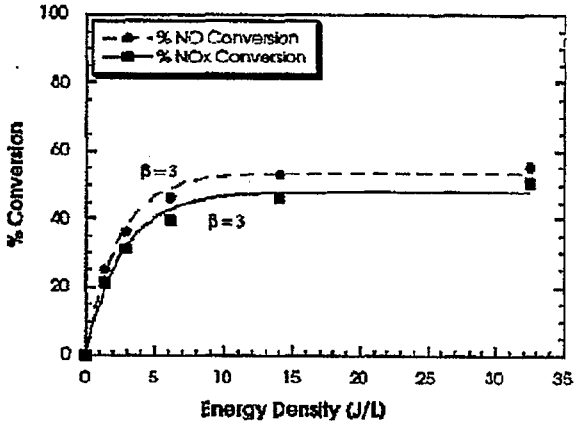

Figure 8b: NO_x destruction efficiency downstream from both the reactor and the catalyst bed.

The production of nitrogen and loss of NO_x was monitored for the two-stage reactor using a gas chromatograph and NO_x meter. Figure 9 shows the area of the nitrogen peak (measured downstream from the catalyst) as a function of time as well as the corresponding chemiluminescent NOx meter reading. At one minute the energy density was increased to 3 J/L and the corresponding nitrogen signal increased while the NOx decreased by 77 ppm (32% conversion). At 25 minutes known quantities of nitrogen were added to the gas mix for nitrogen quantification. After the standard N_2 additions (57 min) the power was increased from 3 J/L to 7.4 J/L. When the power is increased, the nitrogen signal increases and the amount of NOx removed increases to 94 ppm (39% conversion).

At 80 minutes another N_2 standard addition was performed then the plasma power was turned off.

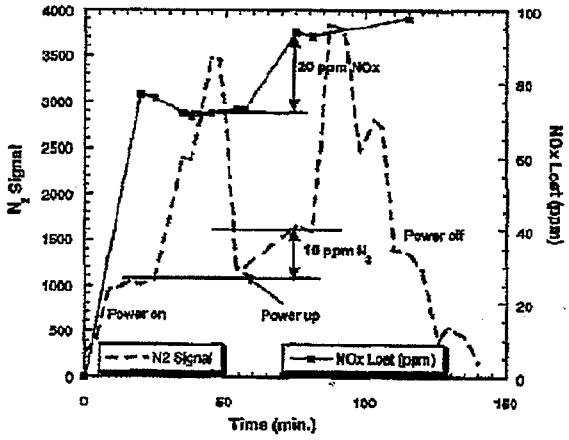

Figure 9: N_2 production measured by a gas chromatograph and NOx loss as measured by the NOx analyzer downstream from a catalyst in the 2-stage configuration with He carrier gas.

The gc response as a function of nitrogen concentration is shown in Figure 10 for standard additions at 3J/L and 10J/L. Considerable variation in the amount of N_2 produced from NOx reduction results from different interpretations of the results. The slope of the calibration line is lower at higher power, again suggesting that there is some N! formation in a helium plasma. Therefore, the calculated amount of NOx converted to N_2 is 44% using the low power (3 J/L) calibration and 56% using the high power (7.4 J/L) calibration. Interestingly, if we calculate the increase in N_2 caused by increasing the power to the reactor, the value exactly matches the increase in NOx conversion. For example when the power is increased from 3 J/L to 7.4 J/L, 10 ppm more N_2 is detected for an additional 20 ppm of NOx converted.

In an attempt to account for all the nitrogen-containing species, the catalysts were subjected to long term plasma tests then analyzed for surface adsorbed species using both temperature programmed desorption and wet chemical analysis. These techniques showed that 13"2% and 7"2% of the total NOx removed is adsorbed to the surface in single-stage and two-stage configurations respectively. While this increases the nitrogen balance to about 84% and 57% for single stage and two-stage configurations respectively, it does not account for all of the missing NO_x.

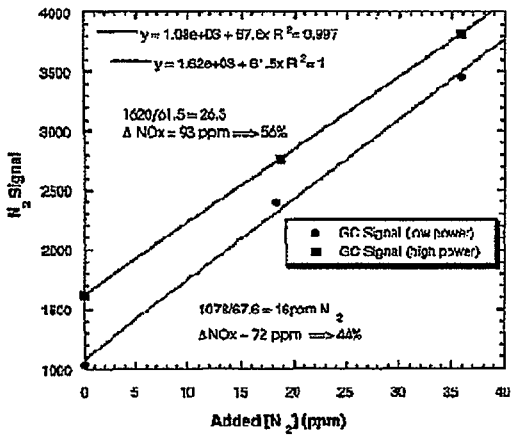

Figure 10: GC signal response as a function on nitrogen concentration for two-stage configuration at two different energy densities.

FTIR spectrometry was used to analyze for other potential nitrogen-containing by products using a parallel plate reactor and the same catalyst. These tests were conducted at Ford Motor Co. and are published in detail elsewhere [6]. The parallel plate reactor without the catalyst did not reduce NO but simply converted it to NO_2, similar to the reactor used in this study. The FTIR monitored for NO, NO_2, N_2O, HONO, HNO_3, and CH_3ONO_2 (methyl nitrate), as well as for hydrocarbon species. With the catalyst, the concentrations of N_2O, HONO, HNO_3, and CH_3ONO_2 were all below the detection limit of the FTIR, which measured an apparent NO_x reduction of 55%. Therefore, the missing NOx that could not be quantified as nitrogen can not be accounted for from by-product formation to these species. However, there may be some other nitrogen-containing species that goes undetected by FTIR. Further work needs to be done to identify potential by-products. It is possible that the NO_x reduction as measured by the FTIR is accurate (i.e. there are no additional nitrogen-containing by-products) and that the nitrogen imbalance is a result of errors in the experimental conditions used to measure and quantify nitrogen. Substantial error in the measurement of the quantity of nitrogen produced could result from small changes in the background nitrogen levels.

As can be seen from Figures 4 and 9, the nitrogen produced from NO reduction increases slowly over time periods of up to 50 minutes until it reaches steady state. Slow release of N_2 from the catalyst surface after the plasma is off or non-steady state conditions when the plasma is on could also act to lower the measured nitrogen produced from NOx reduction.

CONCLUSIONS

Results presented in this paper show that N_2 from NO_x reduction can be measured if background N_2 in simulated diesel exhaust is replaced with helium. Two reactor configurations where the catalyst is contained in the plasma region (single-stage) and where the catalyst is downstream from the plasma (two-stage) both produce N_2 from NOx reduction. Comparison of the amount of N_2 produced as measured directly by the gas chromatograph with the amount of NO_x removed as measured by the chemiluminescent NO_x analyzer shows that 76% and 44-56% of the NO_x removed is reduced to nitrogen for single stage and two-stage configurations respectively. FTIR analysis of product species on a similar plasma/catalyst system with a lean burn mix containing N_2 (no He) did not reveal significant production N_2O, NO_2, HONO, HNO_3, or CH_3ONO_2. In addition, less than 13% of the NOx removed is adsorbed to the catalyst surfaces. Further work is needed to determine if the discrepancy between NO_x reduction as measured by the FTIR and the gas chromatograph is due to undetected nitrogen-containing by-product species, or to inaccuracies in experimental quantification of nitrogen produced from NO_x reduction.

REFERENCES

1. Penetrante, Hsaio, Merritt, and Vogtlin, AFundamental Limits on NO_x Reduction by Plasma,@ SAE Paper 911715, May 1997.

2. Tonkyn, Barlow, Balmer, Orlando, Hoard, and Goulette, AVehicle Exhaust Treatment Using Electrical Discharge methods, A SAE Paper 971716, May 1997.

3. Penetrante, Hsiao, Merritt, and Vogtlin, APlasma-Assisted Heterogeneous Catalysis for NO_x Reduction in Lean-Burn Engine Exhaust,@ in the Proceedings of the 1997 Diesel Engine Emissions Reduction Workshop.

4. Balmer, Tonkyn, Kim, Hoard, Yoon, Jimenez, Orlando, and Barlow, ADiesel NOx Reduction on Surfaces in Plasma,@ SAE paper 982511, 1998.

5. Penetrante, Pitz, Hsiao, Merritt, and Vogtlin, AEffect of Hydrocarbons on Plasma Treatment of NOx,@ in the Proceedings of the 1997 Diesel Engine Emissions Reduction Workshop.

6. Hoard and Balmer, AAnalysis of Plasma-Catalysis for Diesel NO_x Remediation,@ SAE paper 982429, 1998.

EVALUATION OF GAS PHASE PULSED PLASMA EMISSIONS SYSTEM FOR DIESEL EXHAUST AFTERTREATMENT

K. A. Koshkarian and A. Chanda
Caterpillar, Incorporated

Vishwesh Palekar and Madhu Ramavajjala
NOxTech, Incorporated

ABSTRACT

With emissions standards for diesel engines used in on-highway applications becoming increasingly more stringent, the need for exhaust gas aftertreatment becomes more likely. Non-thermal plasmas have received a lot of attention recently as a technology that may hold significant potential for reducing both NOX and particulate matter. Caterpillar, Incorporated and NOxTech, Incorporated have been cooperatively working to evaluate NOxTech's gas phase pulsed power plasma emission system for use in the heavy-duty diesel (HDD) exhaust environment. The system has been tested on a synthetic gas reactor test bench using blended gas that simulates HDD exhaust (without particulates). In addition, preliminary testing of the device utilizing exhaust from a Caterpillar 3406 engine has been performed. Results of the evaluation tests will be presented.

200

Evaluation of Gas Phase Pulsed Plasma Emissions System for Diesel Exhaust Aftertreatment

Kent A. Koshkarian - Caterpillar Inc.
Vish Palekar - NOxTech Inc.

Diesel Engine Emissions Workshop '98
Castine, Maine July 6-9, 1998

CATERPILLAR®

NOXTECH

Background

Program objective:

- **Investigate the diesel engine emissions reduction potential of two non-thermal plasma aftertreatment systems.**

Approach:

- **Develop evaluation techniques and screen NTP device on test bench**
- **Evaluate technology on-engine (if warranted)**

Technologies:

- ***NOxTech - gas phase pulse plasma***
- Tecogen - high speed injection of free radical reagents

★ **Funding provided by DOE**

CATERPILLAR®

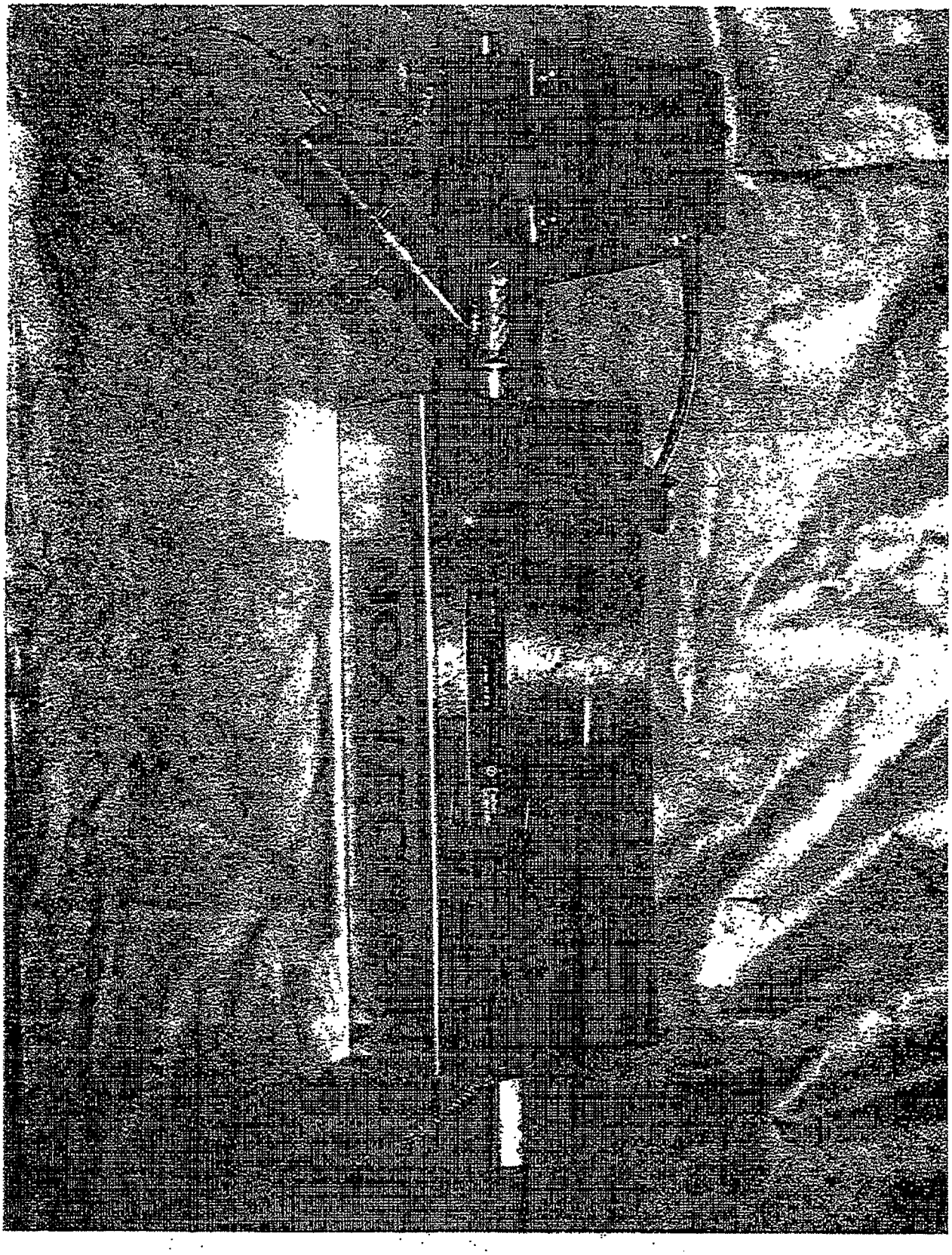

NOxTech Gas Phase Pulse Plasma System

- **Reactor System Details**
  - ▸ Corona discharge type NTP
  - ▸ Reactor volume = 0.3 liters
  - ▸ Gas flow capability = 0-200 liters/minute
  - ▸ Temperature capability = RT-550 C
- **Electrical System Details**
  - ▸ Voltage range = 0-40 KV
  - ▸ Repetition rate = 0-1000 Hz

CATERPILLAR®

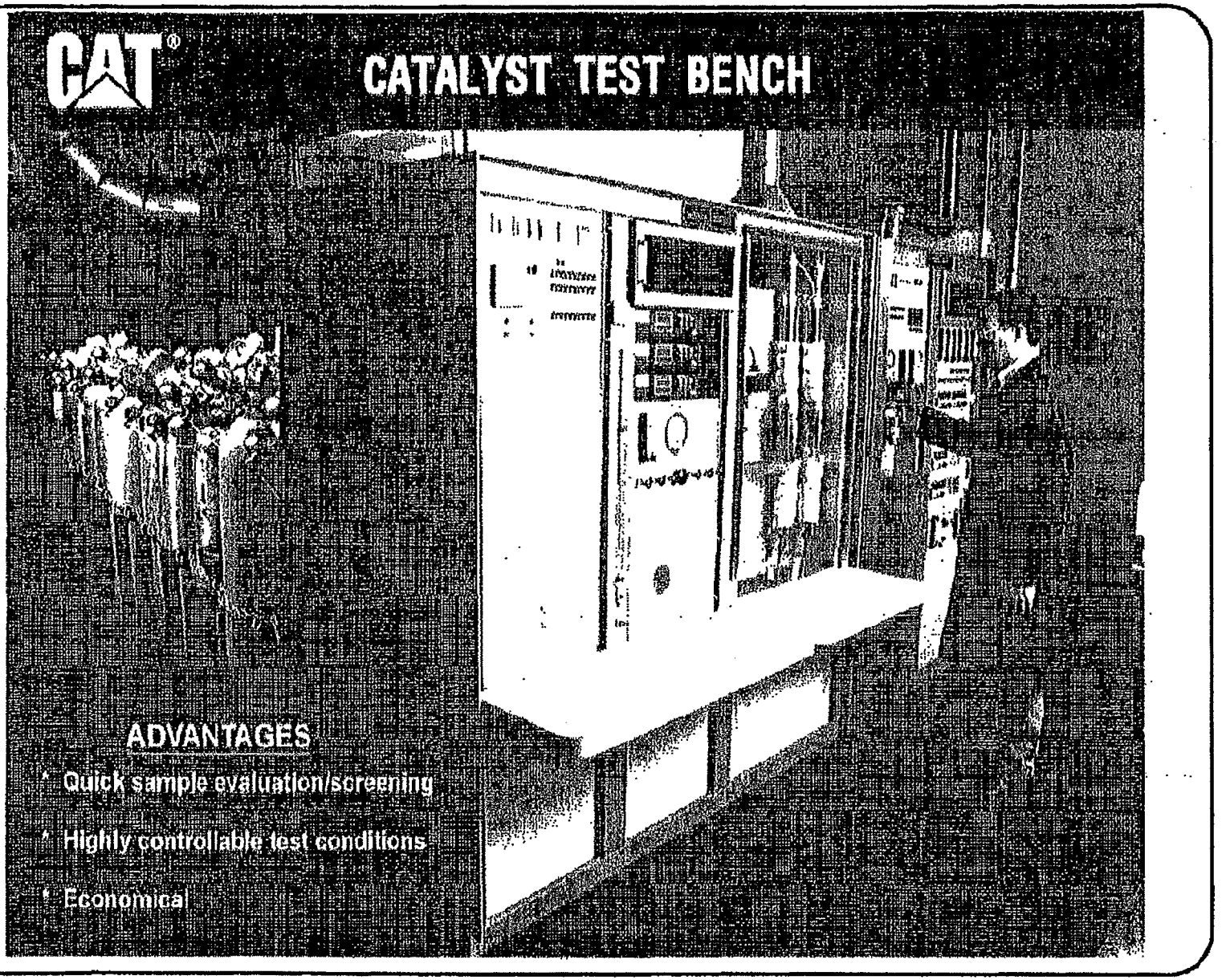

CATERPILLAR

Caterpillar Simulated Exhaust Test Bench

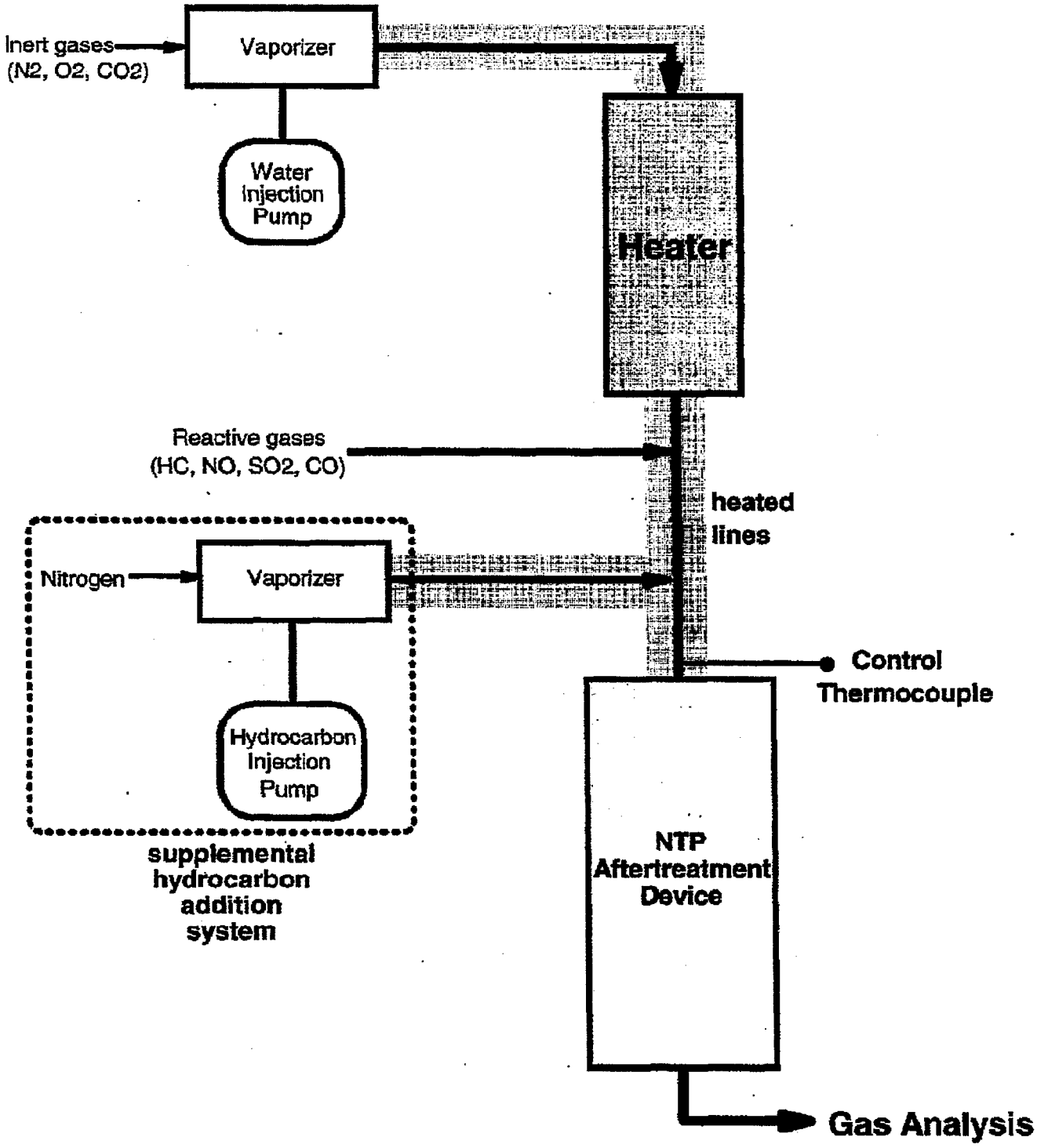

CATERPILLAR®

NTP Device Setup on Reactor Test Bench

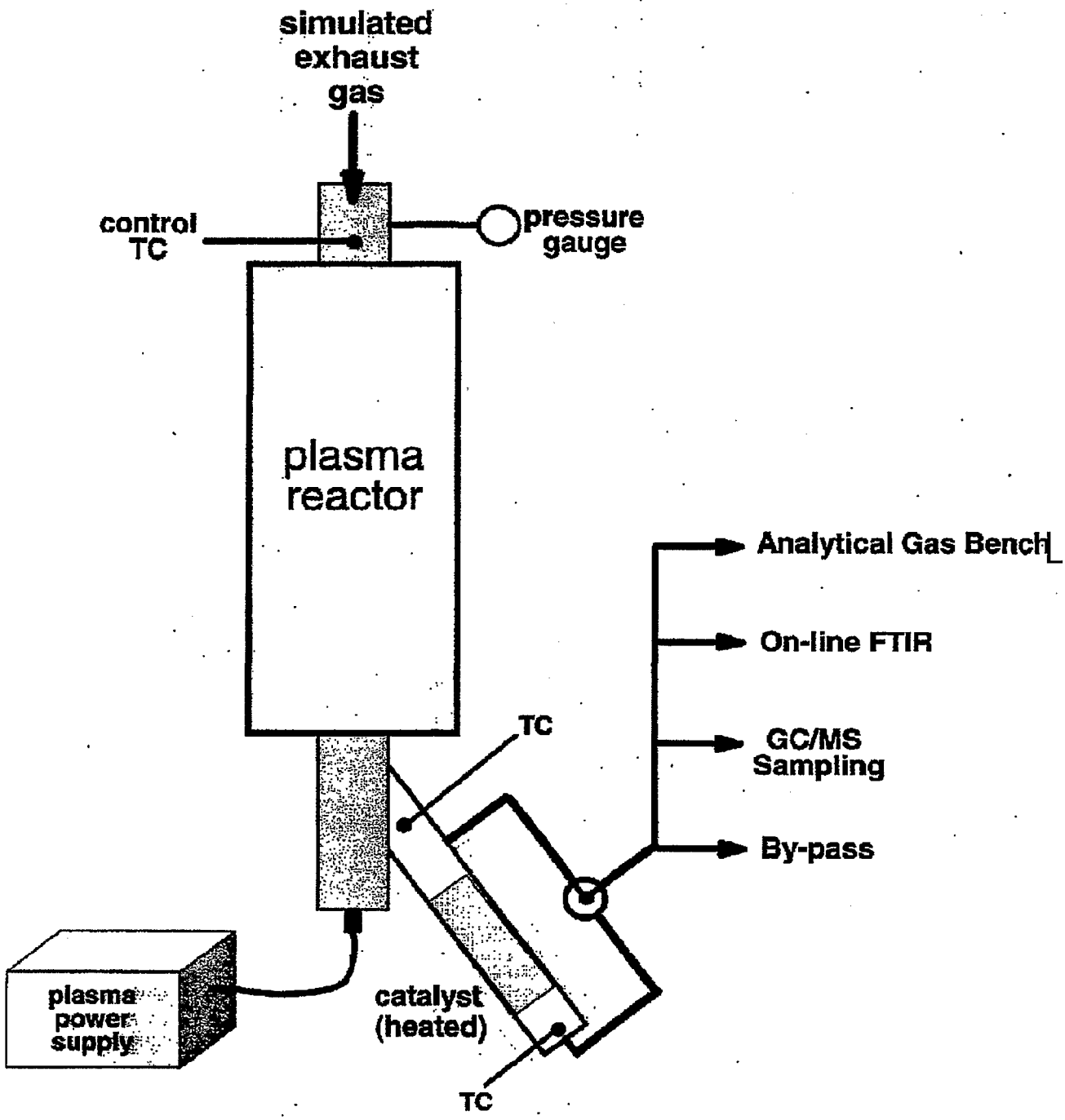

CATERPILLAR

Analysis of Exhaust Species

► Analytical gas bench

- NOx analyzer (chemi)
- HC analyzer (FID)
- CO/CO2 analyzer (NDIR)
- SO2 analyzer (NDIR)
- O2 analyzer (MPA)

► On-line FTIR - Nicolet

- detection and "quantification" of over 20 species

► Gas Chromatograph/Mass Spectrometer

- Using thermal desorption tube sampling
- Detection of unknown species

► Analysis of water condensate

- Ion Chromatography
- Detection of nitrate, nitrite, sulfate, sulfite, and chloride

CATERPILLAR®

FTIR Detectable Compounds

- Nitric oxide (NO)
- Nitrogen dioxide (NO_2)
- Nitrous oxide (N_2O)
- Nitric acid (HNO_3)
- Nitrous acid (HNO_2)
- Ammonia (NH_3)
- Hydrogen cyanide (HCN)
- Methyl Nitrite (CH_3NO_2)

- Ozone (O_3)
- Formaldehyde (HCHO)
- Acetaldehyde (CH_3CHO)

- Carbon monoxide (CO)
- Carbon dioxide (CO_2)
- Water (H_2O)
- Sulfur dioxide (SO_2)

- Methane (CH_4)
- Ethane (C_2H_6)
- Ethene (C_2H_4)
- Propane (C_3H_8)
- Propene (C_3H_6)
- Acetylene (C_2H_2)

Reactor Bench Test Conditions

	Typical engine exhaust conditions	Conditions used for bench tests
CO2 (%)	4 - 9	6
CO (ppm)	50 - 300	200
NO (ppm)	200 - 1600	500
SO2 (ppm)	5 - 30	30
HC (C1 ppm)	10 - 140	500
O2 (%)	7 - 17	9
H2O (%)	5 - 9	7
N2 (%)	balance	balance
Temperature (C)	100 - 600	200 - 450
gas flow (liter/min)	up to 35,000	37.5 - 62.5

CATERPILLAR®

Results of Reactor Bench Testing

- Effect of NOxTech NTP on NOx:
  - NO to NO2 is dominant reaction
  - HNO3 & N2O detected (HNO3 = 8-15 ppm, N2O = 5-10 ppm)
  - Approximately 10-20% of initial NOx unaccounted
    - ★ In condensate ?
    - ★ Undetected species ?
- Effect of NOxTech NTP on NOx when followed by oxidation catalyst:
  - Reconversion of species back to NOx
  - Minor amount of N2O formed
- Wide variety of compounds were observed after the NTP reactor:
  - Formaldehyde, acetaldehyde (20-50 ppm)
  - Ozone (5-8 ppm)
  - Nitric & nitrous acid, nitrous oxide
- Backpressure has an affect on electrical characteristics of the NTP.

Engine Test Setup

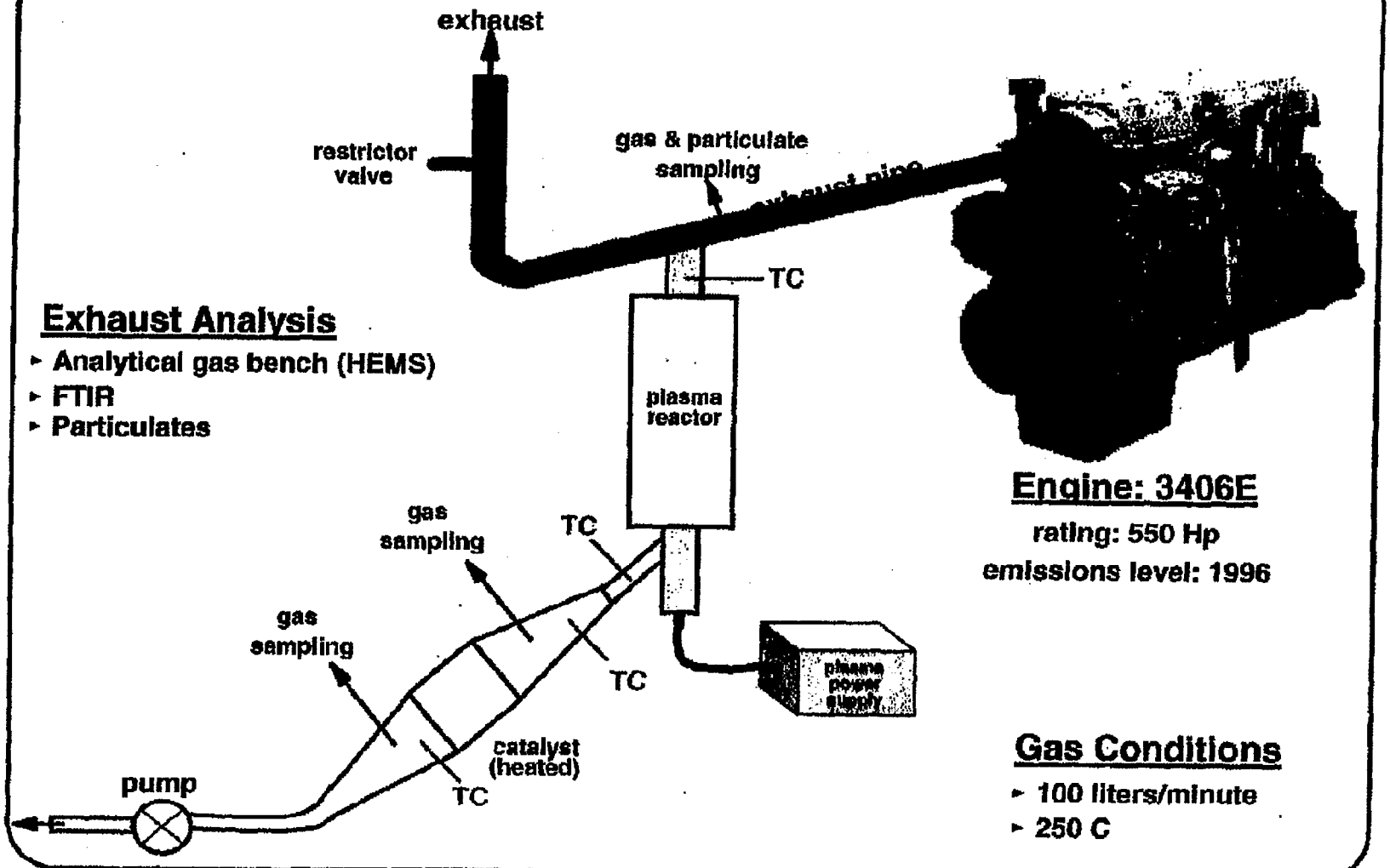

Exhaust Analysis

- Analytical gas bench (HEMS)
- FTIR
- Particulates

Engine: 3406E

rating: 550 Hp

emissions level: 1996

Gas Conditions

- 100 liters/minute
- 250 C

CATERPILLAR®

Preliminary Results of Engine Testing

- Similar trends as observed in reactor bench tests.
  - largely an oxidative process
- Notable differences:
  - less formation of aldehydes
  - greater formation of HNO2, HNO3
  - Ozone not detected
  - Lower energy density
- Tests with downstream oxidation catalyst are incomplete.

Summary

- Preliminary evaluation is near completion.
- Under test conditions used by Caterpillar there appears to be, at best, very minor (<10%) conversion of NOx to nitrogen.
- Effort to accurately detect and quantify all nitrogen containing species is crucial.
- Continuous feedback and discussion of test results with NOxTech.
- Further effort is currently being evaluated.
  - ★ Field test demonstrations are <u>not</u> planned

CATERPILLAR®

PLASMA MUFFLERS FOR NOx ABATEMENT

Victor Puchkarev, Greg Roth, Daniel Erwin,† and Martin Gundersen
University of Southern California
Department of Electrical Engineering-Electrophysics
Los Angeles, California 90089-0484
†Department of Aerospace and Mechanical Engineering
Los Angeles, California 90089-1191

ABSTRACT

This paper reports efficient treatment of diesel emission with transient, non-equilibrium plasma created by a pulsed corona discharge. The transient plasma (~50 ns) is found to reduce NOx emission in a flow of 1-10 liters/second with energy cost ~10-20 eV/molecule, corresponding to a fraction of source power of ~5%. The efficiency of NOx reduction is a complex function of parameters that include pulse width, pulse polarity, current density, repetition rate, and reactor design. It was found that best efficiencies are correlated with a low current density (0.2 A/cm^2) and high repetition rate (1 kHz) under high flow rate. Careful optimization of all these parameters is required to reach cost effective NOx reduction.

INTRODUCTION

Plasma processing for control of effluents from many different sources including diesel engines, incinerators, and power plants is currently receiving considerable attention because these approaches have potentially broad impact on the reduction of harmful gaseous pollutants. For example, the removal of nitrogen oxides (NOx) is an important problem, and has led to rigid regulation on the level of NOx emission [1]. E-beam, pulsed corona, surface and silent discharges have been implemented to study efficiency of NOx removal in many experiments [2]. There are several issues that affect the practical application of pulsed plasma devices including: i) energy cost, ii) byproducts emission, iii) pulsed power implementation, and iv) reactor design. Energy costs that have been reported vary considerably—for example, in terms of energy cost per treated molecule from 3 to 500 eV/molecule (this approach to calculating energy costs is discussed in ref. 2). To be competitive for remediation of diesel engine emission, the energy cost should be <10-20 eV per NOx molecule for concentrations ~1000 ppm, which would correspond to an overall power consumption <5% of the total engine power. Electron beam processing has been reported to have low energy cost [4] following injection of highly energetic electrons—requiring, however, a level of sophistication in implementation that is impractical at present for diesel exhaust treatment. Reactors based on corona and silent discharges have the advantages of relative simplicity, scalability and lower capital cost than existing e-beam technology. Thus it is of interest to understand the physical mechanisms and practical limits to energy cost for this competing, simpler technology. In this paper we present experimental data on NOx reduction from diesel engine exhaust by a corona discharge with an energy cost previously considered attainable only by sophisticated electron beam methods.

EXPERIMENTAL

The experimental apparatus reported here incorporated a discharge chamber, pulsed power modulator, and gas manifold with controller gauges and emission analyzer. A number of reactors were studied; a typical pulsed corona reactor consisted of a cylindrical chamber length of 0.4 m and varying diameter—inner electrode 2-34 mm and outer electrode 20-62 mm. It was possible to vary the current density and "active" plasma volume by varying the electrode surface area. The reactor cathode surface was typically threaded to ensure a high local electric field with increasing radius. The current density entering the plasma volume was estimated for a nominal cylinder surface 1 mm above the surface of central electrode. The term "active" plasma volume is used to mean the volume which is within this cylindrical surface (e.g. volume enclosing the maximum electric field). The active plasma volume can be visually detected at high frequency as a bright plasma core a few mm away from the hot electrode surface.

The pulse generator supplied high voltage pulses with amplitude ~40 kV, pulse duration of 50-100 ns (rise time 20 ns), and repetition rate up to 1 kHz. In early experiments pulses reflected from an unmatched load (the reactor and discharge)

were absorbed in a matched pulse generator load. Then we found that pulses reflected from unmatched modulator load contributed between 5 to 20% of energy input main pulse, so in further experiments we used modulator with unmatched load. By monitoring voltage and current signals related to the discharge it was possible to determine the energy deposition into the gas. The total current contains both the discharge current and the current associated with charging the capacitance of the reactor. The product of the discharge current and voltage during the corona discharge yields the pulse energy *E*. The energy cost ε was calculated as:

$$\varepsilon = \frac{250 \bullet E \bullet f}{F \bullet \Delta NOx} [eV / molecule]$$

where f is the frequency in Hz, F is the flow rate in liter/s, and ΔNOx is the NOx reduction in ppm. The power input into the discharge was varied as a function of pulse length, voltage amplitude and repetition rate. Typical current and voltage oscillograms during discharge are shown in Figure 1.

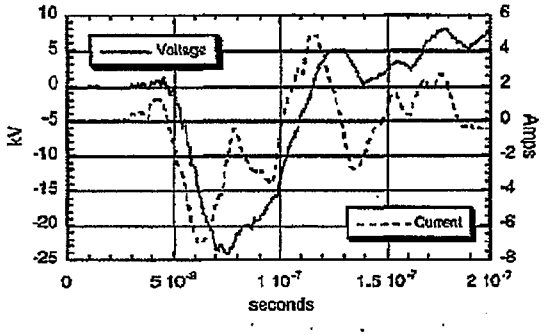

Figure 1. A Typical Voltage/Current Trace for the Corona Discharge Reactor

Three sets of experiments using different diesel engines were conducted:

I. Initial experiments used a 60 kW engine (Volkswagen Rabbit) operated at idle speed and NO emission concentrations of 100-130 ppm. Here the exhaust temperature was 40-50° C. We monitored the outlet gas composition using an electrochemical NO analyzer (Bacharach, Nonoxor II). No other species concentrations were measured.

II. Subsequent testing used a 300 kW engine operated under load with high NO emission (600-1000) ppm. Exhaust temperature was varied from 85 to 180° C. A Horiba analyzer was used for the emission monitoring. This system allowed detection of the following components: NO, NO_2, HC, CO, CO_2, SO_2 [3].

III. Recent experiments were performed with a 10 kW diesel motor generator and variable electrical load. Emission was monitored using a portable electrochemical LANCOM flue gas analyzer. Typical emission constituents and their concentrations are: CO – (400-800) ppm, CO2 – (2-4)%, NO – (120-400) ppm, NO2 – (30-60) ppm, CxHx – 120-600 ppm, O2 – (14-18)%. Here high values in concentration of exhaust constituents refer to a loaded engine.

Depending on the reactor dimension the flow rate was varied between 100 and 1500 standard liters per minute (flow velocity in reactor was between 1 to 8 m/s).

EXPERIMENTAL RESULTS

On varying discharge parameters (pulse width, voltage amplitude, frequency, pulse polarity) it was found that the energy cost changes considerably, and that short pulses (~50 ns) are more advantageous in energy cost than longer pulses, in part because short pulses allow operation with a higher pulse voltage during the time of treatment of the effluent. We found that the energy cost for NO removal is affected by pulse polarity. The energy cost for positive corona (plus at the central electrode) is 1.5-2 times that for negative charging of the central electrode. This is because positive corona carries higher current at a given pulse voltage than negative, though NOx reduction was almost the same, and current is found here to be a crucial parameter for determining of energy cost. Data hereafter refer to negative corona and pulse duration of 50 ns.

We performed experiments to compare the efficiency of pulsed corona discharges with and without a dielectric insert under otherwise identical experimental conditions. As a dielectric insert we used ceramic cylinder adjoined to the outer electrode. The voltage amplitude and the frequency were adjusted in such a way that these approaches could be compared for the same level of NO reduction. It was found unexpectedly that the dielectric insert results in higher current (conductive current, rather than displacement one) and current density. Reduction of NO is approximately equal, but energy cost with the dielectric insert is 2-3 times greater than for the discharge without dielectric. We discuss reason of this effect later.

The high repetition rate regime is found to be advantageous for both cases. It was also found

in our data that the energy cost decreases with increasing frequency. Energy cost lowering occurs basically due to the decrease of energy per pulse with increasing of repetition rate.

Table 1. Emission and energy cost data obtained with 300 kW engine.

Item	240 A/300 Hz Conc., ppm In	Out	Energy Cost eV/mol	40 A/1 kHz Conc., ppm In	Out	Energy Cost eV/mol
NOx	1160	1010	30	970	900	18
NO	1060	790	17	890	770	10
NO_2	100	220		80	130	
CO	303	352		303	350	
CO_2%	0.12	0.12		0.12	0.12	
HC	110	66		110	66	

Table 1 and Table 2 list selected experimental data obtained in the different sets of experiments. Despite the variety of experimental conditions (engines, reactor design), and analyzing units (electrochemical and chemiluminescent) we found that with optimal energy deposition into the gas, energy effective NOx/NO destruction by pulsed corona is feasible.

Table 2. Energy parameters and NOx/NO reduction for various experimental conditions.

Flow (l/sec)	4	4	2.4	2.4
f (Hz)	1000	2000	1000	300
Ep (J/p cm^3)	3E-5	1.8E-5	8.8E-5	15E-5
E* (J/cm^3)	2.5E-3	3E-3	12E-3	6.3E-3
eNOx (eV/mol)	7.2	8	23	21
eNO (eV/mol)	3.9	4.6	16	10
ΔNOx (ppm)	84	97	113	70
ΔNO (ppm)	152	167	180	152
ΔNOx/ΔNO_2	1.24	1.38	1.63	0.86

Ep is the specific input energy per pulse per cm^3, E* is the total specific energy, e is the energy cost for NOx, and NO. ΔNOx and ΔNO are NOx and NO reduction in absolute values (ppm). The last row is the ratio of ΔNOx reduction to ΔNO_2 production (ΔNOx/ΔNO_2).

Figure 2 summarizes experimental data obtained in all sets of experiments with various reactors, and varying pulse parameters and flow rate. Most of the data were obtained in the first set of experiments — this is why the data are plotted on NO removal–energy cost coordinates. To estimate total NOx reduction one divides the NO value roughly by 1.8. The goal of this figure is to illustrate how the important parameters – the NO removal and energy cost – are unpredictably related to each other. Careful optimization of experimental conditions resulted in maximum NO reduction at reasonable energy cost.

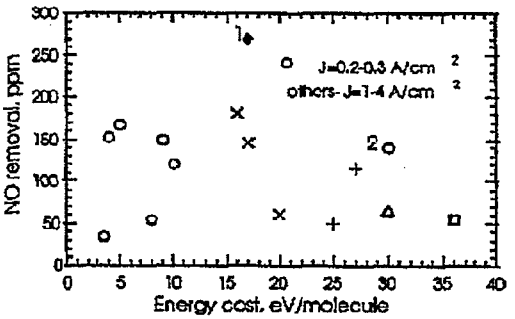

Figure 2. Total NO Removal as a Function of Energy Cost for Various Experimental Conditions

The most important figure of merit is specific energy deposition in gas (J/liter =Ep times the number of pulses, see table 2). It follows from Table 2 that the energy-effective regime is achieved at E*~ 2-3 J/liter. The energy input is related basically to the pulsed current, and current shows rapid growth with voltage. However, NO/NOx removal increases more slowly resulting in increasing energy cost (see Table 2); therefore, we also plotted the energy cost vs. pulsed current density (Figure 3). This figure seems to be confusing as the extrapolation to zero current density (input energy) results in the maximum efficiency. There should be an optimum in the energy input (current density). The clue, most likely, is in the corona discharge uniformity, and we discuss this later. Another cause for optimal energy input is the competition between remediation reactions and radical recombination [4].

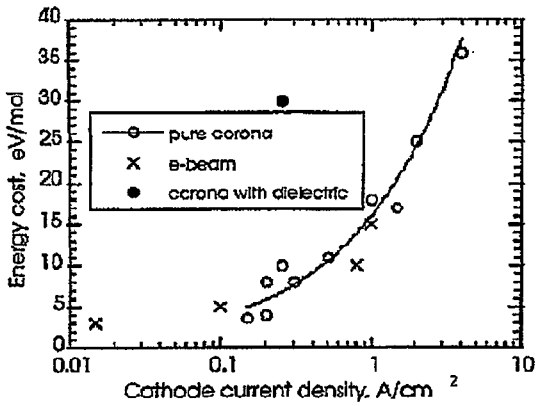

Figure 3. Energy Cost Against the Current Density for Various Experimental Conditions.

1) Reactor with increased "active" plasma volume [9], current density 1.5 A/cm^2. 2) Reactor with dielectric insert; diameter of inner electrode 34 mm, the inner diameter of ceramic tube 58 mm.

At a given energy cost (e.g. at 5-10 eV/molecule) maximum NO removal is proportional to the initial NO and HC concentration, and 'active' plasma volume (reactor design). We also believe that NOx removal and energy cost depends on particulate matter concentration, which is varied for different engines. For example, we found that a blocking mechanical filter in upstream of reactor resulted in lower NOx removal and increased the energy cost by a factor of 2-3.

The maximum NOx removal obtained in the set III experiments was between 100 to 120 ppm (about 30%), with energy cost below 10 eV/molecule. This it appears is a limit for a given reactor and pulsed power conditions. As an effective regime is limited by optimum specific energy input into the gas (which must be small enough) the only way to increase the percentage of NOx removal is to increase the 'active' plasma volume.

DISCUSSION

Plasma aftertreatment of diesel exhaust principally relies on the removal of nitrogen oxides (NOx) and other hazardous components by highly reactive radicals produced in corona discharge by energetic electrons. During the high voltage short pulse, energetic electrons and radicals are generated and subsequently initiate chemical reactions. For this, pulsed parameters (voltage amplitude and pulse width) must be optimized in accordance with the reactor design, and it is observed that these depend in subtle ways on small variations in design. Short pulse excitation is followed by a post-pulse period, which lasts, from 10s of microseconds to 100s of ms or longer [4]. During this time various remediation and oxidation reactions occur, which are as yet not well characterized, although calculated optimal time intervals for post-pulse chemical reactions are ~1 ms [4].

The chemical reactions occur mainly in the gas phase, but the plasma composition and characteristics can be affected by heterogeneous reactions of ions, electrons, and radicals. These reactions can considerably decrease the energy cost. For example, the lowest energy cost – several eV per molecule – has been measured using e-beam for SO_2 decomposition [5,6]. The authors found that the energy consumption is affected by pulse duration [5] and current density [6] decreasing with decreasing current density. Further, Deminskii et al. [7] discussed the kinetics of a heterogeneous oxidation process which involves chemical reactions between gas and aerosol particles with consideration of dissolved components, transfer processes in gas and liquid, and the dynamics of the formation and decay of aerosol particles. They found good agreement with experimental data and predicted even less energy cost ~0.3 eV/molecule. In this work we attempted to study the relation between current density and energy cost for corona discharge-based reactors. Figure 3 shows the energy cost of NO reduction plotted as a function of current density.

Thus the energy cost of NO removal by pulsed corona discharge is also driven by current density similar to e-beam processing of SO_2 [5,6]. Reactor 2 with a dielectric insert, despite the low current density exhibits however much higher energy cost. We had anticipated increased NO reduction with low energy cost because this reactor had big plasma volume and large area cathode: the ratio of inner-to-outer electrode diameter was 0.58 (34 - 58 mm). Here the dielectric barrier was supposed to prevent arcing. Despite that, we found that discharge trends to contract into bright filaments at high repetition rate. This might be due to the fact that the volume resistivity of alumina ceramic rapidly drops with temperature; thus local area heating could produce current filamentation.

One should note that the uniform plasma is a major problem of corona discharge. Due to a strong nonlinear dependence of field emission on the local electric field the number of starting streamers is an extremely sensitive function of electric field and cathode microgeometry, which is hard to control. It is likely that at high current, the current is carried by a finite number of filaments, rather than being equally distributed over the

cathode surface. Thus the energetic electrons are generated only in the streamers whose volume is a mall part of the total gas volume (in the limit the current can flow through a single channel). This can explain the effect of pulse polarity on energy cost. The streamer velocity is higher for a positive hot electrode, which results in strong current filamentation. It was visually observed that at low current and current density the plasma is more uniformly distributed over the electrode surface than at high current. A high repetition rate and flow appears to help smoothing the current irregularities. This result is still the subject of further study.

In pulse corona discharge NO is partly converted into NO_2. The production of NO_2 was found to vary with current density, and be minimal at a low current density ~0.2 A/cm^2, corresponding also to energy efficient operation of the reactor (see tables 1 and 2).

There are two key pathways for NO removal:

Reduction: $NO + N \rightarrow N_2 + O$

And

Oxidation: $NO + O/O_3 \rightarrow A$; $NO/NO_2 + OH/HC \rightarrow A$;

here A - are various species.

The first reaction is most desirable and according to ref. 4 has the highest rate constant. However recent experiments [10,11] indicate that only 5 to 20% remediation of NO occurs via reduction.

We have recently initiated a series of experiments to study the spatial and temporal distribution of NO (25-50 ppm in a dry air) in a single streamer using laser-induced fluorescence (LIF). We found that NO depletion occurs in a close proximity to and along the streamer channel. Within a few milliseconds following pulsed excitation NO destruction occurs. Thus NO remediation may occur slowly, rather than in a few ten's of microseconds [4]. This is also implies the presence of an oxidation process.

Chemistry in heterogeneous media [7] may also have significant and sometimes beneficial effects for oxidation. It was found that there is a higher energy cost for hot exhaust 180°C, above the vaporization temperature for water, corresponding to elimination of droplets. A similar result was previously reported [8]. Hydrocarbons are favorable for NO/NO_2 oxidation but considerably increase the pathways for various byproduct productions.

SUMMARY

Energy cost measurements of NO-NOx removal from diesel exhaust with a pulsed corona discharge has been experimentally studied. After optimization of pulsed parameters (polarity, pulse width) we found that the energy cost is driven by current decreasing with corresponding current density decrease. Best efficiency (<10 eV/molecule) is obtained at current density <0.2 A/cm^2 and repetition rate (~1 kHz). With increasing current density (energy deposition into gas) the removal efficiency decreases. Our results indicate that a pulsed corona discharge provides effective NO remediation with energy cost comparable to e-beam processing. The spatial and temporal characteristics of streamer discharge impose limitations on the removal efficiency at high NO concentration so that reactor design is an important consideration. Another issue that needs studying is a thorough analysis of by-products generated by plasma reactor.

Acknowledgment: It is a pleasure to acknowledge D. Walker for making possible diesel testing arrangements at Golden West College. This work was supported by grants from the Office of Naval Research, the Army Research Office, the National Science Foundation, and the Powell Foundation.

REFERENCES

1. J. J. Brogan, *Abstracts of Diesel Engine Emissions Reduction Workshop*, (July 24-25, San Diego, California) p. A3. 1995.

2. A collection of articles on various plasma technologies and on efficiency of different methods for plasma remediation of toxic gases appears in *Non-Thermal Plasma Techniques for Pollution Control*, Part A and Part B, edited by B.M. Penetrante and S.E. Schultheis, (Springer, New York 1993).

3. Experiments with 300 kW engine and emission analysis were performed under the direction of D. Walker at the Diesel Technology Laboratory, Golden West College, and Huntington Beach, CA Beach.

4. A. C. Gentile and M. J. Kushner, J. Appl. Phys. 78, 2074, (1995).

5. D L Kuznetsov, G.A. Mesyats and Yu. N. Novoselov, "Influence of the pulse duration of ionizing e-beam on the efficiency of removal of SO_2 from smokestack gases" Tech. Phys. Lett. 20, 269, (1994).

6. B.V. Potapkin, M. A. Deminskii, A. A. Fridman, and V. D. Rusanov, in book *Non-Thermal Plasma Techniques for Pollution Control*, Part A, edited by B.M. Penetrante and S.E. Schultheis, (Springer, New York 1993), pp. 91-106.

7. M. A. Deminskii, B.V. Potapkin, V. D. Rusanov, , "The Kinetic of Nonequilibrium Chain Plasma-Chemical Oxidation in Heterogeneous Media" and A. A. Fridman, High Energy Chemistry **28**, 304, (1994).

8. E. M. van Veldhuizen, W. R. Rutgers, and V. A. Bityurin, "Energy Efficiency of NO Removal by Pulsed Corona Discharges", Plasma Chemistry and Plasma Processing **16**, 227, (1996).

9. M. Gundersen, V. Puchkarev, I. Yampolsky, US Patent #5 603 893 (1997).

10. Marnix A. Tas, R. van Hardeveld, and E. M. van Veldhuizen, "Reactions of NO in a Positive Streamer Corona Plasma", Plasma Chemistry and Plasma Processing, Vol.17 (4), pp.371-391, (1997).

11. T. Hammer, S. Broer, and T. Kishimoto, "Pulsed excitation of Silent Discharges for Diesel Exhaust Treatment", Abstract of 4th Intern. Conf. On Advanced Oxidation Technologies for Water and Air Remediation, Orlando, Florida, Sept. 23-26, 1997.